



*IDENTIFICATION OF MOLECULAR TARGETS OF
SWERTISIN IN GLUCOSE HOMEOSTASIS, ISLET
DIFFERENTIATION & FUNCTIONALITY*

CHAPTER 3



Chapter 3: Identification of molecular targets of Swertisin in glucose homeostasis, islet differentiation & functionality

Chapter 3: Identification of molecular targets of Swertisin in glucose homeostasis, islet differentiation & functionality

3.1 Introduction

A state of hyperglycemia is a hallmark characteristic of diabetes mellitus. Sustaining good glycaemic control is a pre-requisite of any effective diabetes therapy. B cells of pancreatic islets are the major target of antidiabetic drugs causing normoglycemia through insulin secretagogue activity. Apart from other organs, kidney plays a key role in maintaining normoglycemia in blood. Sodium glucose co-transporter 2 (SGLT2) is responsible for 97 % and SGLT1 for 3 % reabsorption of glucose. However, this mechanism becomes malabsorptive in diabetes (Novikov and Vallon 2016) and hence hyperglycemia persists. Hyperglycemia also affects certain protein kinases that are involved in the regulation of SGLT (Haneda, Araki et al. 1997) (Lee, Lee et al. 2007)

SGLT2 inhibitors are highly explored current class of drugs not only in type 2 diabetes but also in type 1 diabetes as its mechanism is independent of circulating insulin or insulin sensitivity (Novikov and Vallon 2016). Gliflozins are commercially available SGLT2 inhibitors for the management of high glucose levels. Gliflozins like canagliflozin, dapagliflozin, empagliflozin inhibit the reabsorption of glucose in the kidney, thereby causing excretion of glucose in the urine (glucosuria) (Nespoux and Vallon 2018). Apart from SGLT2 inhibition, other potential actions have also been attributed to this class of drugs. One of the SGLT2 inhibitors, empagliflozin treatment was found to be related to improved β -cell function in type 2 diabetic patients and preserving β -cell mass in type 1 diabetes in mice model studies (Al Jobori, Daniele et al. 2018) (Cheng, Chen et al. 2016). On the other side, canagliflozin also improves β -cell function in patients with type 2 diabetes (Polidori, Mari et al. 2014). Hamamatsu et al. demonstrated that diabetic mice treated with canagliflozin significantly preserved β -cell mass (Hamamatsu, Fujimoto et al. 2019). So gliflozins have beneficial effects on pancreatic β -cells apart from inhibiting SGLT2. The important role of the natural compound phlorizin in the development of SGLT inhibitors has been extensively reported. Besides phlorizin, various flavonoids and especially flavonoid enriched plant

Chapter 3: Identification of molecular targets of Swertisin in glucose homeostasis, islet differentiation & functionality

extracts have been explored for their glucose lowering effect targeting SGLT2. Phlorizin and naturally available flavonoid glycosides have paved the way for the development of various C glycosides and their analogs (Ghezzi, Loo et al. 2018) (Jesus, Vila-Viçosa et al. 2017) (Blaschek 2017).

One such bioactive, swertisin, a C-glucosyl flavone has been extracted from a medicinal plant *Enicostemma Littorale* (EL). Our Lab has shown has demonstrated glucose lowering activity if swertisin in STZ induced diabetic mice (Srivastava, Dadheech et al. 2018). Our Lab explored its potent islet neogenic property from pancreatic progenitors/Bone marrow derived mesenchymal stem cells (Dadheech, Soni et al. 2013) (Dadheech, Srivastava et al. 2015) (Nidheesh Dadheech Ph.D Thesis) (Mitul Vakani Ph.D Thesis). In the current chapter of the present thesis, Swertisin being a C-glucosyl flavone has been explored for SGLT2 inhibition using the target prediction tool (Daina, Michielin et al. 2019) and *in silico* analysis. We have explored various metabolic alterations associated with the application of swertisin in both *in vitro* and *in vivo* diabetic models. We have elucidated the role of swertisin in establishing a link between its glucose lowering action and SGLT2 inhibition and proved it an excellent antidiabetic drug.

3.2 Materials and Methods

3.2.1 *In silico* molecular target identification of swertisin in glucose lowering effect

A. *In silico* pharmacokinetic study of swertisin

To study the time profile of absorption, distribution, metabolism, and excretion (ADME) of swertisin, we initiated our experimental studies with *in silico* clinical pharmacokinetics. We also found the toxicity (T) potential of swertisin. For pharmacokinetics and drug-likeness analysis of swertisin in the human system, an *in silico* approach using the ADMETlab tool was used that calculate ADMET properties using principles of 3DQSAR (Quantitative Structure–Activity Relationship) and 3DQSPR (Quantitative Structure–Property Relationship).

B. *In silico* target prediction of swertisin

To study the potential activity of swertisin that confers such rapid blood glucose lowering effect, *in silico* target prediction of swertisin was done. We performed two types of analysis:

Chapter 3: Identification of molecular targets of Swertisin in glucose homeostasis, islet differentiation & functionality

1. Target prediction studies were done using the Swiss Target Prediction tool (<http://www.swisstargetprediction.ch/>) (Daina, Michielin et al. 2019).
2. PASS (Prediction of Activity Spectra for Substances) Analysis of Swertisin was performed (<http://www.pharmaexpert.ru/passonline/predict.php>).

C. Homology modeling and preparation of human SGLT2 protein structure

Due to the lack of crystal structure of human SGLT2 isoform in PDB (Protein Data Bank), we proceeded with homology modelling of SGLT2 using the I-TASSER server (Yang, Yan et al. 2015) (Zhang 2008). I-TASSER is a web based, full chain protein prediction server used for protein modelling (Fig 3.1). It first scans a representative PDB structure library to search for possible folds by threading the target sequence using Profile-profile threading alignment (PPA). Models having conformational similarities are clustered. After clustering the structure decoys, the lowest energy structure in each cluster is chosen. The confidence of each model is quantitatively measured by C-score which is typically in the range of [-5, 2], where a C-score of a higher value signifies a model with a higher confidence and vice-versa.

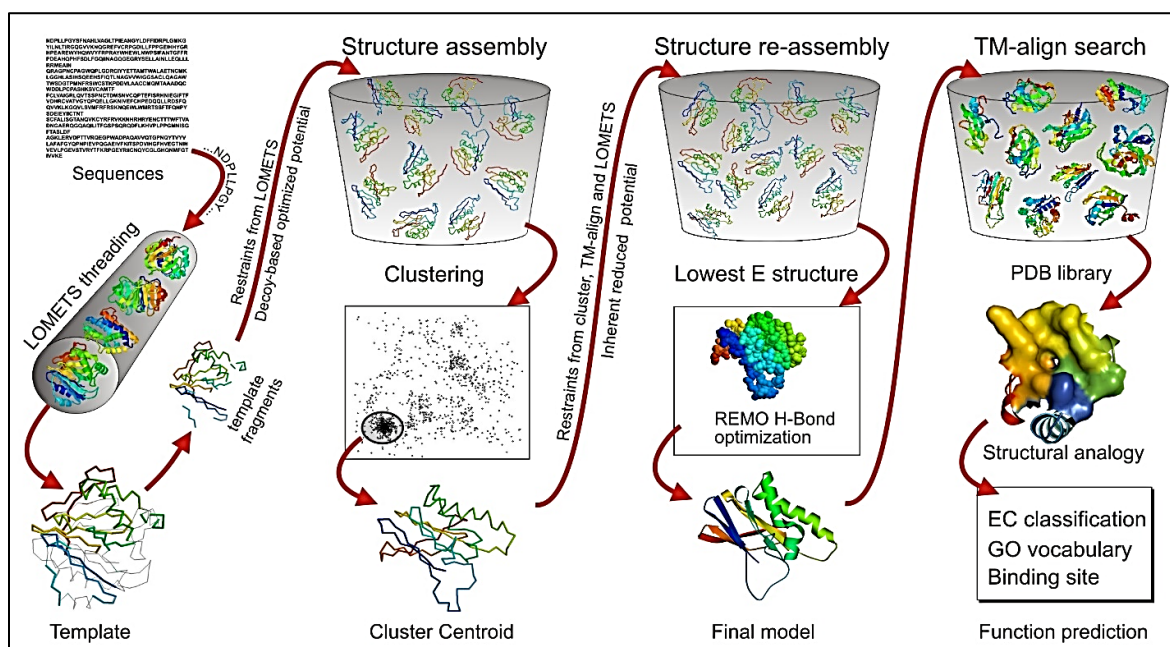


Figure 3.1 I-TASSER protocol for protein structure and function prediction (Roy, Kucukural et al. 2010, Yang, Yan et al. 2015)

Chapter 3: Identification of molecular targets of Swertisin in glucose homeostasis, islet differentiation & functionality

D. Structure Validation of the Human SGLT2 (hSGLT2) model

I-TASSER server provided five structures for each of the target proteins and the one with the best C-Score was chosen. The PROCHECK program (<https://www.ebi.ac.uk/thornton-srv/software/PROCHECK/>) and was used further to check the structure quality of the predicted model from I-TASSER. Structural validation of the target proteins model was done to determine stereochemical aspects along with main chain and side chain parameters, which shows that most of the residues of modelled hSGLT2 structure falling under allowed, favoured and disallowed regions of a Ramachandran plot obtained from PROCHECK RAMPAGE software (Lovell, Davis et al. 2003) (<http://mordred.bioc.cam.ac.uk/~rapper/rampage.php>).

E. Molecular docking of hSGLT2 with swertisin

Molecular docking is a computational procedure that attempts to predict bound conformations and free energies of binding for small molecule ligands to macromolecular targets.

Energy minimized hSGLT2 structure was used for molecular docking. The coordinates for Swertisin (CID: 124034) and Canagliflozin (CID: 24812758) were downloaded from the PubChem database (Kim, Chen et al. 2019). The ligands were minimized with CHARMM forcefield using Discovery Studio v.20 for 2000 max steps and with Momany-Rone partial charge estimation. The ligands (Swertisin and Canagliflozin) and receptor (hSGLT2) used for molecular docking were prepared using AutoDock Tools 4.2 graphical interface (Morris, Huey et al. 2009). The PDB coordinates were converted to PDBQT format which includes added charges, if necessary, merging non-polar hydrogens, and assigning appropriate atom types. Affinity (grid) maps were generated by placing the center of the grid near active site residues. For molecular docking, the AutoDock Vina program (Trott and Olson 2010) was used. The docked complexes were analyzed using Discovery Studio Visualizer (Fig 3.2).

Chapter 3: Identification of molecular targets of Swertisin in glucose homeostasis, islet differentiation &
functionality

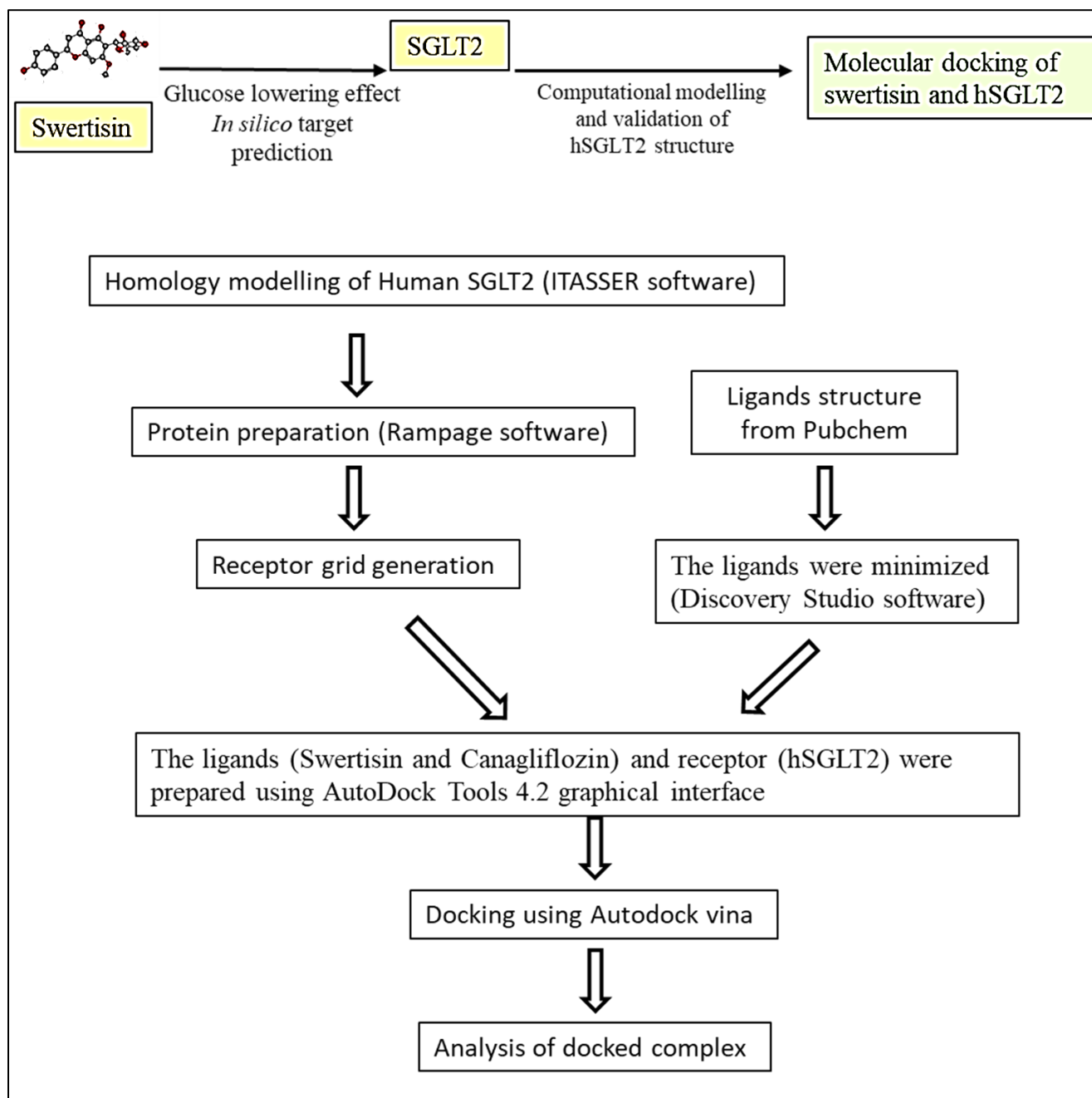


Figure 3.2 *In silico* plan of work for molecular docking of swertisin

Chapter 3: Identification of molecular targets of Swertisin in glucose homeostasis, islet differentiation & functionality

F. Molecular dynamics simulation of hSGLT2 and hSGLT2 docked complexes

For accessing the binding stability of the apo-protein SGLT2 and SGLT2 in complex with swertisin as well as SGLT2 complex with known reference canagliflozin, MD simulations (MDS) were performed (Chaudhari, Chaudhari et al. 2021) (Manhas, Patel et al. 2019) (Patel, Patel et al. 2018) (Patel, Athar et al. 2020) (Patel, Athar et al. 2021) (Patel, Parmar et al. 2017, Vora, Patel et al. 2020). A set of three MDS (SGLT2; SGLT2-swertisin; and SGLT2-canagliflozin) were prepared and calculations were conducted for the time duration of 100 ns each using GROMACS 2020.5 (Abraham, Murtola et al. 2015). For all the MDS, Gromos43a1 force-field was used (Pol-Fachin, Fernandes et al. 2009). For parameterization of swertisin and canagliflozin, PRODRG2 server was used (Schüttelkopf and van Aalten 2004).

All the MDS systems were solvated with simple point charge (SPC) water model in dodecahedron box maintaining a distance of 1 nm edge from the center of the protein. The system was neutralized with an equal number of counter ions (Na^+/Cl^-) as required. Simulations were subjected to energy minimization using the steepest descent algorithm to generate maximum force below 1000 $\text{kJmol}^{-1} \text{ nm}^{-1}$ (50000 max steps) for removing steric clashes and bad contacts. Further NVT (constant number [N], constant volume [V] and constant temperature [T]) and NPT (constant number [N], constant pressure [P] and constant temperature [T]) ensemble equilibration was performed with position restraint for 1 ns each. The modified Berendsen thermostat algorithm (Berendsen, Postma et al. 1984) was used for NVT equilibration and Parrinello-Rahman barostat (Parrinello and Rahman 1980) was used for NPT equilibration. For long-range electrostatic interactions Particle Mesh Ewald approximation (Darden, York et al. 1993) was used with 1 nm cut-off. Cut-off of 1 nm was used for computing coulombic and the van der Waals interactions and the bond length was constraint using the LINCS algorithm (Hess, Bekker et al. 1997). Finally, 100 ns production run was conducted with coordinates saved at every 2 fs time-step with similar parameters as stated above. The post MDS analysis was carried out using tools available within GROMACS for root mean square deviation (RMSD), root mean square fluctuation (RMSF), and hydrogen bonds (H-bonds). The plotting tool GRACE was used for the generation and visualization of the plots. To assess the collective motion and dynamics of $\text{C}\alpha$ backbone atoms

Chapter 3: Identification of molecular targets of Swertisin in glucose homeostasis, islet differentiation & functionality

during the simulations, essential dynamics analysis or principal component analysis (PCA) and Dynamical Cross-Correlation Matrix (DCCM) was carried out using Bio3D package (Grant, Skjærven et al. 2021).

G. Binding free energy estimation of SGLT2 with swertisin and canagliflozin complexes

The calculations of the binding free energy for protein-ligand complexes is generally carried out by MM-PBSA or molecular-mechanics based generalized Born and surface area (MM-GBSA) continuum solvation methods. The binding free energy calculations defines the quantitative estimation of the swertisin and canagliflozin affinity towards SGLT2. The widely recognized g_mmpbsa tool with default parameters was used for molecular mechanics potential energy (electrostatic + the Van der Waals interactions) and free energy solvation (polar + nonpolar solvation energies) calculations (Kumari, Kumar et al. 2014). Based on the RMSD plots, 200 frames from the last 50 ns trajectory were employed for binding free energy estimation. These frames were selected after the regular interval of 200 ps to cover different conformational states of the systems for better structure-function correlation.

3.2.2 *In vitro* studies

A. Chemicals

Swertisin was previously isolated and stored from the whole dried plant of *Enicostemma littorale* as reported (Dadheech, Soni et al. 2013, Dadheech, Srivastava et al. 2015, Srivastava, Dadheech et al. 2018). Canagliflozin was commercially purchased as INVOKANA® (Janssen).

B. Cell culture

HEK293 and Caco2 cell lines were propagated at 37 °C in 5% CO₂ in DMEM high glucose (Gibco#12100-046) supplemented with 1.0% of penicillin-streptomycin (Gibco#15140-122) and 10% FBS (Gibco#10270-106).

C. Sodium dependent glucose uptake assay

Fluorescence microplate analysis

10,000 cells of HEK 293 or Caco2 were plated in 96-well plates. After 24h preincubation, cells were washed with sodium free buffer (140mM choline chloride, 5mM KCl, 2.5 mM CaCl₂, 1mM

Chapter 3: Identification of molecular targets of Swertisin in glucose homeostasis, islet differentiation & functionality

MgSO₄, 1mM KH₂PO₄, and 10mM HEPES (pH 7.4, adjusted with 2.5M Tris). Cells were serum starved and then preincubated with 0, 7.5, 15, 30 and 40 µg/ml swertisin for 15 min to which was added 2-NBDG (Invitrogen#N13195) in sodium buffer (Sodium buffer contained 140mM NaCl instead of choline chloride), sodium free buffer, and sodium buffer with 10 µM cytochalasin B (MP Biomedical#195119) (GLUT inhibitor) (Kanwal, Singh et al. 2012) for 60 min. After 60 min, the buffers were removed and the cells were rinsed in sodium free buffer and lysed with cold lysis buffer (1% Nonidet P-40, 1% sodium deoxycholate, 40 mM KCl, 20 mM Tris, pH 7.4). The fluorescence intensity was detected on Biotek Synergy HT (USA) microplate reader (Excitation: 485/20, Emission: 528/20). To measure DNA, Hoechst (Himedia#TC266) was added and fluorescence intensity was measured (Excitation: 360/40, Emission: 460/40). 30 µM canagliflozin was taken as a positive control (Hawley, Ford et al. 2016) (Fig 3.3).

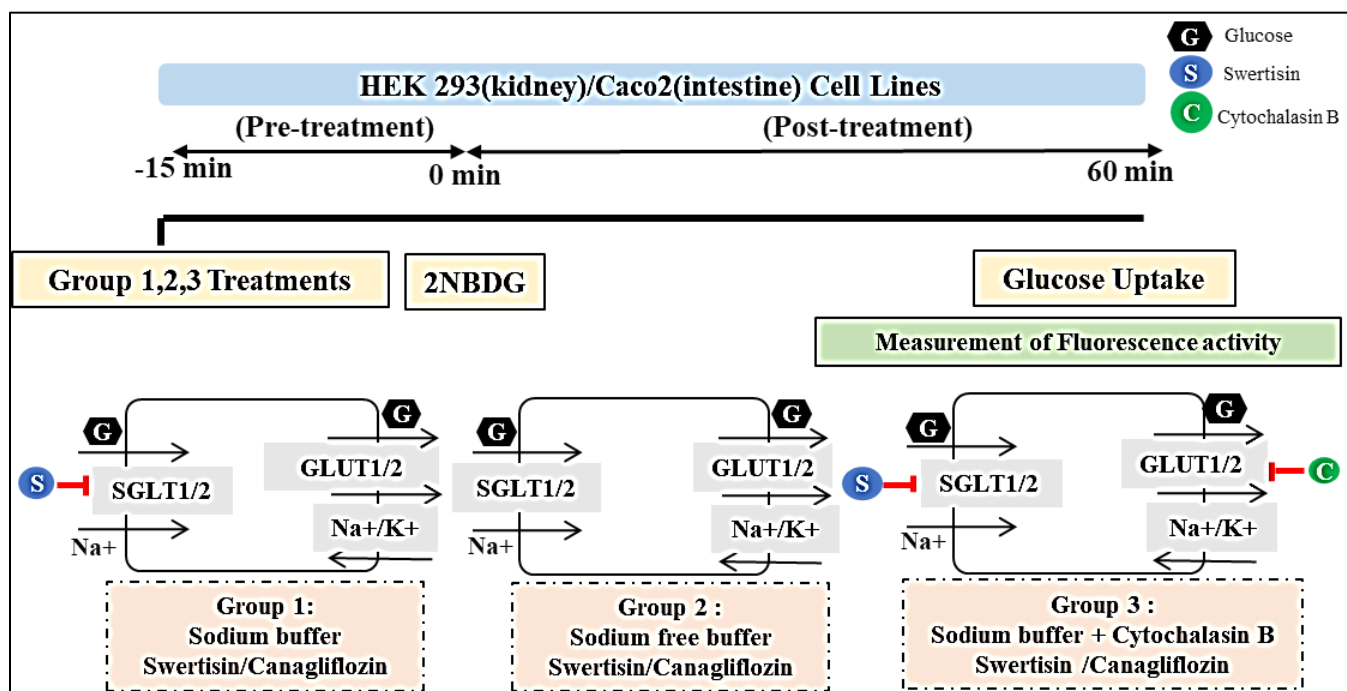


Figure 3.3 *In vitro* plan of work for Sodium dependent glucose uptake

Chapter 3: Identification of molecular targets of Swertisin in glucose homeostasis, islet differentiation & functionality

Fluorescence microscopic analysis

0.5x 10⁶ cells of HEK293 cell line was seeded in 35mm cell culture dish was grown about 80% confluent. Cells were washed with sodium free buffer thrice after aspiration of cell culture media. Cells were then preincubated for 15 minutes with and without 7.5 µg/ml swertisin in sodium buffer with 10 µM cytochalasin B. 100µM of 2-NBDG was added and Live cell imaging was performed with "Objective Lens" "UPLSAPO 20X", "Objective Lens Mag." "20.0X" and "Objective Lens NA" "0.75" under a confocal microscope (FV3000 Olympus, USA) with incubation at 37°C and 5% CO₂. Cells without swertisin treatment were considered as control.

3.2.3 Protein extraction and western blotting

HEK293 cells or Kidney tissues were harvested and kept on ice. Minced tissue powder or harvested cell lysate were lysed in Laemmli lysis buffer. Total protein concentration was estimated by Bradford's method and 20 µg or 15 µg of total protein were resolved and transferred to nitrocellulose membrane for tissues and cells respectively. After blocking was performed for 1 h, blots were subsequently probed with SGLT2 (Abcam#37296), PKC (Millipore#07-264), pp38MAPK (Cell Signalling#9216), ERK1/2 (Cell Signalling#9102), and Beta-actin (BD bioscience#612657) primary antibodies overnight at 4 °C. Blots were then incubated with respective secondary antibodies conjugated with HRP for 1 h at RT. Specific bands of proteins were visualized using enhanced chemiluminescence (ECL) reagent (Bio-Rad) and images were captured on Alliance 4.7 UVI Tec Chemidoc (Uvitech, Cambridge) gel documentation system. Densitometric analysis was carried out by Image J software.

3.2.4 *In vivo* studies

Animal selection and induction of diabetes and *in vivo* experimental design

6–8 weeks old adult male BALB/c mice were kept at the animal house with 12 H light and dark cycle with water and pellet diet ad libitum. These studies were carried out in strict accordance as per the guidelines and approval of the institutional Committee for the Purpose of Control and Supervision on Experiments on Animals, India (CPCSEA) (Protocol no. MSU/BC/IAEC/2016/04). After successfully inducing diabetes with STZ injection (65 mg/kg body weight) for 5 days, the Fasting Blood Glucose of animals was confirmed using Accu-check

Chapter 3: Identification of molecular targets of Swertisin in glucose homeostasis, islet differentiation & functionality

Performa glucometer (Accu-check, Roche, USA) at regular intervals to monitor their diabetic status. After establishing the STZ induced diabetic mice model, mice were divided into four groups control, diabetic, swertisin, and canagliflozin treatment. Each group had 8 to 12 mice each. STZ diabetic mice were treated with swertisin (2.5 mg/kg body weight) and other group treated with canagliflozin (10 mg/kg body weight) from 0 day of experiment till the 15th day. Swertisin was administered with saline intraperitoneally. On the penultimate day of the study, mice from each experimental group were individually housed in metabolic cages by gradual acclimatization with 12 H light and dark cycle with water and pellet diet ad libitum (Fig 3.4). Data were collected in the morning (07:00 H). Animal weight, water, chow consumption, and urine volume were recorded and urine specimens were taken for analysis. Proteinuria was analysed. Serum and urine samples were analysed for urea and creatinine using Reckon diagnostics P. LTD.(India) kits. For the endpoint oral glucose tolerance test, glucose tolerance was monitored by taking blood glucose reading at regular intervals until 2 H.

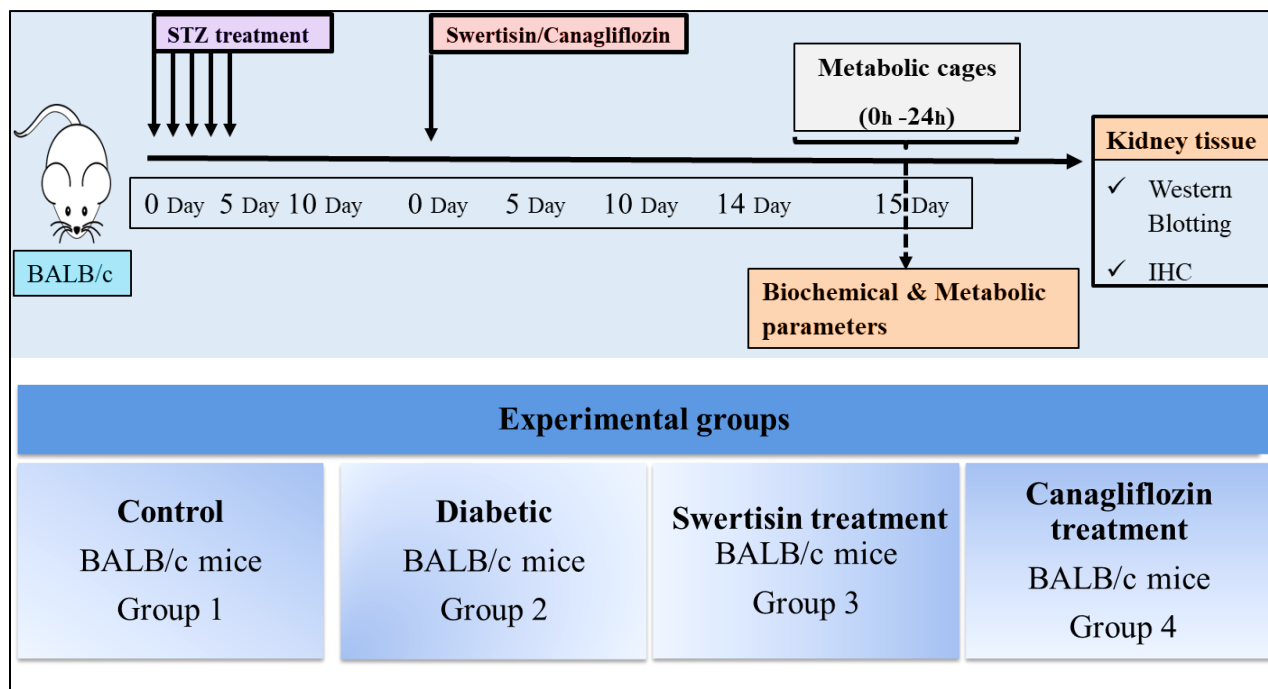


Figure 3.4 Figure showing schematic *in vivo* plan of work

Chapter 3: Identification of molecular targets of Swertisin in glucose homeostasis, islet differentiation & functionality

3.2.5 Immunohistochemistry

The paraffin embedded kidney tissues were preheated at 80°C for 2h. After deparaffinization sections were rehydrated using Xylene for 5 min and varying alcohol grades of 100% for 5 min and 95%, 70%, 50%, for 2 min each and distilled water for 10 min. The slides were put in 0.01 M sodium citrate buffer under boiling conditions. After the slides were cool down for 20 min they were dipped in tap water for 10 min and then dipped in washing buffer. Each section was then incubated in blocking solution at room temperature for 1 hour. Primary antibody SGLT2 (Abcam#37296), were incubated overnight at 4°C. After washing three times with PBS for 10 min, Alexa Flour (CF555) conjugated secondary antibody were incubated for 1 hour at room temperature then counterstained with DAPI, washed with PBS, mounted with coverslips and viewed under a confocal microscope (Zeiss LSM 710).

3.2.6 H&E (Haematoxylin and eosin) staining

The pancreatic, kidney and intestine sections were brought to slide using suitable adhering agent and stained with H&E staining kit (Rapid H&E kits, Bio Lab diagnostics, India). Slides were slightly warmed to melt the wax and removed it with xylene. Xylene was removed with propanol. They were dipped in RAPID NUCLEAR STAIN for 60 secs followed by washing. 3 drops of Scottle tap water buffer was added and washed after 10 mins. Slides were then stained with the eosin stain. Sections were cleared with propanol and then with xylene and mounted with DPX and microscopically viewed (Nikon Instruments Inc.)

3.2.7 Statistical analysis

The data is represented as Mean \pm SEM. The significance of difference was evaluated by the Student's t-test or ANOVA by Graphpad prism 7 or Microsoft Excel.

Chapter 3: Identification of molecular targets of Swertisin in glucose homeostasis, islet differentiation &
functionality

3.3 RESULTS

3.3.1 *In silico*

A. Pharmacokinetic analysis of swertisin

Owing to limited study on pharmacokinetics of swertisin, we initiated our study by *in silico* pharmacokinetic distribution. To study the time profile of absorption, distribution, metabolism, and excretion (ADME) of swertisin, *in silico* clinical pharmacokinetics approach was used to ensure safe and effective therapeutic management of swertisin. ADME analysis describes the disposition of a candidate drug molecule within an organism and influences the kinetics of drug exposure to the tissues (Dong, Wang et al. 2018). We also found the toxicity (T) potential of swertisin. Variables used to characterize toxicity include therapeutic index and median dose lethality (LD₅₀).

**Exploring metabolically compromised secretome and bioactives on islet differentiation and function
for effective diabetic therapy**

Gurprit Bhardwaj Ph.D. Thesis 2022

Chapter 3: Identification of molecular targets of Swertisin in glucose homeostasis, islet differentiation & functionality

Property	Predicted values	Suggestions	Meaning & Preference
PHYSICOCHEMICAL PROPERTY			
LogS (Solubility)	-3.441 log mol/L(161.708 µg/mL)	> 10 µg/ml	Optimal: higher than -4 log mol/L <10 µg/mL: Low solubility; 10–60 µg/mL: Moderate solubility; >60 µg/mL: High solubility
LogD7.4 (Distribution Coefficient D)	0.029	1~5	< 1: Solubility high; Permeability low by passive transcellular diffusion; Permeability possible via paracellular if MW < 200; Metabolism low. 1 to 3: Solubility moderate; Permeability moderate; Metabolism low. 3 to 5: Solubility low; Permeability high; Metabolism moderate to high. > 5: Solubility low; Permeability high; Metabolism high.
LogP (Distribution Coefficient P)	0.395	0~3	Optimal: 0< LogP <3 LogP <0: poor lipid bilayer permeability. LogP >3: poor aqueous solubility.
ABSORPTION PROPERTIES			
Papp (Caco-2 Permeability)	-6.367 cm/s	> -5.15 cm/s	Optimal: higher than -5.15 Log unit or -4.70 or -4.80
Pgp-inhibitor	0.834, Cat-1		Category 0: Non-inhibitor; Category 1: Inhibitor; The Pgp-inhibitor & non-inhibitor classification criteria refers the reference.

**Exploring metabolically compromised secretome and bioactives on islet differentiation and function
for effective diabetic therapy**

Gurprit Bhardwaj Ph.D. Thesis 2022

Chapter 3: Identification of molecular targets of Swertisin in glucose homeostasis, islet differentiation & functionality

Pgp-substrate	0.041, Cat-0		Category 0: Non-substrate; Category 1: Substrate; More likely to be a Pgp substrate: $N+O \geq 8$; $MW > 400$; Acid with $pK_a > 4$ More likely to be a Pgp non-substrate: $N+O \leq 4$; $MW < 400$; Acid with $pK_a < 8$
HIA (Human Intestinal Absorption)	0.254, Cat-0		Category 0: HIA-; Category 1: HIA+; $\geq 30\%$: HIA+; $< 30\%$: HIA-
F (20% Bioavailability)	0.546, Cat-1		Category 0: F20-; Category 1: F20+; $\geq 20\%$: F20+; $< 20\%$: F20-
F (30% Bioavailability)	0.27, Cat-0		Category 0: F30-; Category 1: F30+; $\geq 30\%$: F30+; $< 30\%$: F30-
DISTRIBUTION PROPERTIES			
PPB (Plasma Protein Binding)	79.77%	90	Significant with drugs that are highly protein-bound and have a low therapeutic index.
VD (Volume Distribution)	-0.858 L/kg	0.04~20	Optimal: 0.04-20L/kg; Range: < 0.07 L/kg: Confined to blood, bound to plasma protein or highly hydrophilic; 0.07-0.7L/kg: Evenly distributed; > 0.7 L/kg: Bound to tissue components (e.g., protein, lipid), highly lipophilic.

**Exploring metabolically compromised secretome and bioactives on islet differentiation and function
for effective diabetic therapy**

Gurprit Bhardwaj Ph.D. Thesis 2022

Chapter 3: Identification of molecular targets of Swertisin in glucose homeostasis, islet differentiation & functionality

BBB (Blood– Brain Barrier)	0.183, Cat-0		Category 0: BBB-; Category 1: BBB+; BB ratio ≥ 0.1 : BBB+; BB ratio < 0.1 : BBB- These features tend to improve BBB permeation: H-bonds (total) $< 8-10$; MW $< 400-500$; No acids.
METABOLISM			
P450 CYP1A2 inhibitor	0.174, Cat-0		Category 0: Non-inhibitor; Category 1: Inhibitor; Molecules that labelled inhibitor in PubChem BioAssay were regarded as inhibitor.
CYP450 1A2 substrate	0.42, Cat-0		Category 0: Non-substrate; Category 1: Substrate; Molecules that labelled substrate in PubChem BioAssay were regarded as substrate. Characteristics of CYP1A2 substrate: $0.08 < \text{LogP} < 3.61$; Planar amines and amides
CYP450 3A4 inhibitor	0.283, Cat-0		Category 0: Non-inhibitor; Category 1: Inhibitor; Molecules that labelled inhibitor in PubChem BioAssay were regarded as inhibitor. Strategies to Reduce CYP3A4 Inhibition: Decrease the lipophilicity (LogD 7.4); Add steric hindrance to the heterocycle para to the nitrogen; Add an electronic substitution (e.g., halogen) that reduces the pKa of the nitrogen.
CYP450 3A4 substrate	0.444, Cat-0		Category 0: Non-substrate; Category 1: Substrate; Molecules that labelled substrate in PubChem BioAssay were regarded as substrate. Characteristics of CYP3A4 substrate: $0.97 < \text{LogP} < 7.54$; Large molecules

**Exploring metabolically compromised secretome and bioactives on islet differentiation and function
for effective diabetic therapy**

Gurprit Bhardwaj Ph.D. Thesis 2022

Chapter 3: Identification of molecular targets of Swertisin in glucose homeostasis, islet differentiation & functionality

CYP450 2C9 inhibitor	0.105, Cat-0		Category 0: Non-inhibitor; Category 1: Inhibitor; Molecules that labelled inhibitor in PubChem BioAssay were regarded as inhibitor.
CYP450 2C9 substrate	0.54, Cat-1		Category 0: Non-substrate; Category 1: Substrate; Molecules that labelled substrate in PubChem BioAssay were regarded as substrate. Characteristics of CYP2C9 substrate: $0.89 < \text{LogP} < 5.18$; Acidic (Nonionized)
CYP450 2C19 inhibitor	0.173, Cat-0		Category 0: Non-inhibitor; Category 1: Inhibitor; Molecules that labelled inhibitor in PubChem BioAssay were regarded as inhibitor.
CYP450 2C19 substrate	0.387, Cat-0		Category 0: Non-substrate; Category 1: Substrate; Molecules that labelled substrate in PubChem BioAssay were regarded as substrate.
CYP450 2D6 inhibitor	0.321, Cat-0		Category 0: Non-inhibitor; Category 1: Inhibitor; Molecules that labelled substrate in PubChem BioAssay were regarded as substrate.
CYP450 2D6 substrate	0.498, Cat-0		Category 0: Non-substrate; Category 1: Substrate; Molecules that labelled substrate in PubChem BioAssay were regarded as substrate. Characteristics of CYP2D6 substrate: $0.75 < \text{LogP} < 5.04$; Basic (Ionized)
ELIMINATION			
T 1/2 (Half Life)	1.479 h	> 0.5	Range: >8h: high; 3h < Cl < 8h: moderate; <3h: low
CL (Clearance)	1.314 mL/min/kg		Range: >15 mL/min/kg: high; 5mL/min/kg < Cl < 15mL/min/kg: moderate; <5 mL/min/kg: low

**Exploring metabolically compromised secretome and bioactives on islet differentiation and function
for effective diabetic therapy**

Gurprit Bhardwaj Ph.D. Thesis 2022

Chapter 3: Identification of molecular targets of Swertisin in glucose homeostasis, islet differentiation & functionality

TOXICITY			
hERG (hERG Blockers)	0.45, Cat-0		Category 0: Non-blockers; Category 1: Blockers; Where molecules with IC ₅₀ < 40 µM were regarded as blockers. Features may lead to hERG blocker: A basic amine (positively ionizable, pK _a >7.3). Hydrophobic/lipophilic substructure(s) (ClogP >3.7). Absence of negatively ionizable groups or oxygen H-bond acceptors.
H-HT (Human Hepatotoxicity)	0.512, Cat-1		Category 0: H-HT negative(-); Category 1: H-HT positive(+); The H-HT positive(+) & negative(-) classification criteria refers the reference.
AMES (Ames Mutagenicity)	0.518, Cat-1		Category 0: Ames negative(-); Category 1: Ames positive(+); Ames positive(+) & negative(-): significantly induces revertant colony growth at least in one out of usually five strains, otherwise, negative.
SkinSen (Skin sensitization)	0.212, Cat-0		Category 0: Non-sensitizer; Category 1: Sensitizer; Sensitizer & Non-sensitizer: The (r)LLNA experimental value. (r)LLNA: (Reduced) local lymph node assay.
LD50 (LD50 of acute toxicity)	3.115 log mol/kg (342.556 mg/kg)	> 500 mg/kg	Median lethal dose (LD50) usually represents the acute toxicity of chemicals. It is the dose amount of a tested molecule to kill 50 % of the treated animals within a given period. High-toxicity: 1~50 mg/kg; Toxicity: 51~500 mg/kg; low-toxicity: 501~5000 mg/kg.

Chapter 3: Identification of molecular targets of Swertisin in glucose homeostasis, islet differentiation & functionality

DILI (Drug Induced Liver Injury)	0.672, Cat-1		Category 0: DILI negative(-); Category 1: DILI positive(+); The DILI positive(+) & negative(-) classification criteria refers the reference.
FDAMDD (Maximum Recommended Daily Dose)	0.608, Cat-1		Category 0: FDAMDD negative(-); Category 1: FDAMDD positive(+); The FDAMDD positive(+) & negative(-) classification criteria refers the reference.

Table 3.1 *In silico* pharmacokinetic analysis demonstrating Absorption, Distribution, Metabolism, Elimination and Toxicity analysis of swertisin by ADMETLab

Chapter 3: Identification of molecular targets of Swertisin in glucose homeostasis, islet differentiation & functionality

The solubility of swertisin is predicted as -3.441 log mol/L and -4.036 log mol/L for canagliflozin which shows that swertisin has higher solubility than canagliflozin since the optimal solubility values should be higher than -4.0 log mol/L. The distribution co-efficient (LogD_{7.4}) is 0.029 for swertisin suggesting high solubility, low permeability and low metabolism as contrast to 2.471 for canagliflozin which shows moderate solubility, moderate permeability and low metabolism. LogP (Distribution Coefficient P) is 0.395 for swertisin pointing towards optimal and 2.968 for canagliflozin suggesting poor aqueous solubility. The absorption parameters of swertisin were at par with canagliflozin. Papp (Caco-2 Permeability) -6.367 cm/s which is low permeability. Pgp-inhibitor value is 0.834 which stands positive for being an inhibitor and value for Pgp-substrate is 0.041. which suggests that swertisin is a non-substrate for Pgp. Human Intestinal Absorption 0.254 indicating very poor intestinal absorption. While in distribution canagliflozin is shown to cross blood brain barrier while swertisin do not cross it. While in metabolism swertisin is a substrate for CYP450 2C9 among all the other cytochromes. While canagliflozin is a CYP450 2C19 inhibitor and CYP450 2D6 substrate Swertisin has a low T_{1/2} (Half Life) of 1.479 h and a low CL (Clearance) of 1.314 mL/min/kg. Under toxicity parameters it is not a hERG blockers and does not have skin sensitization while canagliflozin is a hERG blocker. Swertisin and canagliflozin shows human hepatotoxicity and Drug Induced Liver Injury. The Maximum Recommended Daily Dose is 0.608 and 0.556 for canagliflozin. The LD₅₀ (LD₅₀ of acute toxicity) is 342.556 mg/kg for swertisin. It is the dose amount of a tested molecule to kill 50 % of the treated animals within a given period which is low in case of swertisin. Based on the values obtained, Swertisin exhibits low absorption, moderate metabolism and a low clearance rate. Moreover, Swertisin demonstrates moderate drug-likeness and follows Lipinski's rule. Compared to all other commercially available gliflozins, toxicity of Swertisin is mild, is cardio-protectant and not a skin-irritant. (Table 3.1).

Chapter 3: Identification of molecular targets of Swertisin in glucose homeostasis, islet differentiation & functionality

B. Molecular target prediction of swertisin

SwissTargetPrediction software narrowed the results to Sodium Glucose Cotransporter Class Protein as one of the targets of swertisin. This online tool allows to estimate the most probable macromolecular targets of bioactive small molecule. The prediction is founded on a combination of 2D and 3D similarity with a large number of proteins from different species. SwissTargetPrediction is based on the so-called 'similarity principle' that two similar bioactive molecules are likely to share their protein targets. The predicted targets are those having the actives displaying the highest similarity with the query molecule (Fig 3.5) (Table 3.2).

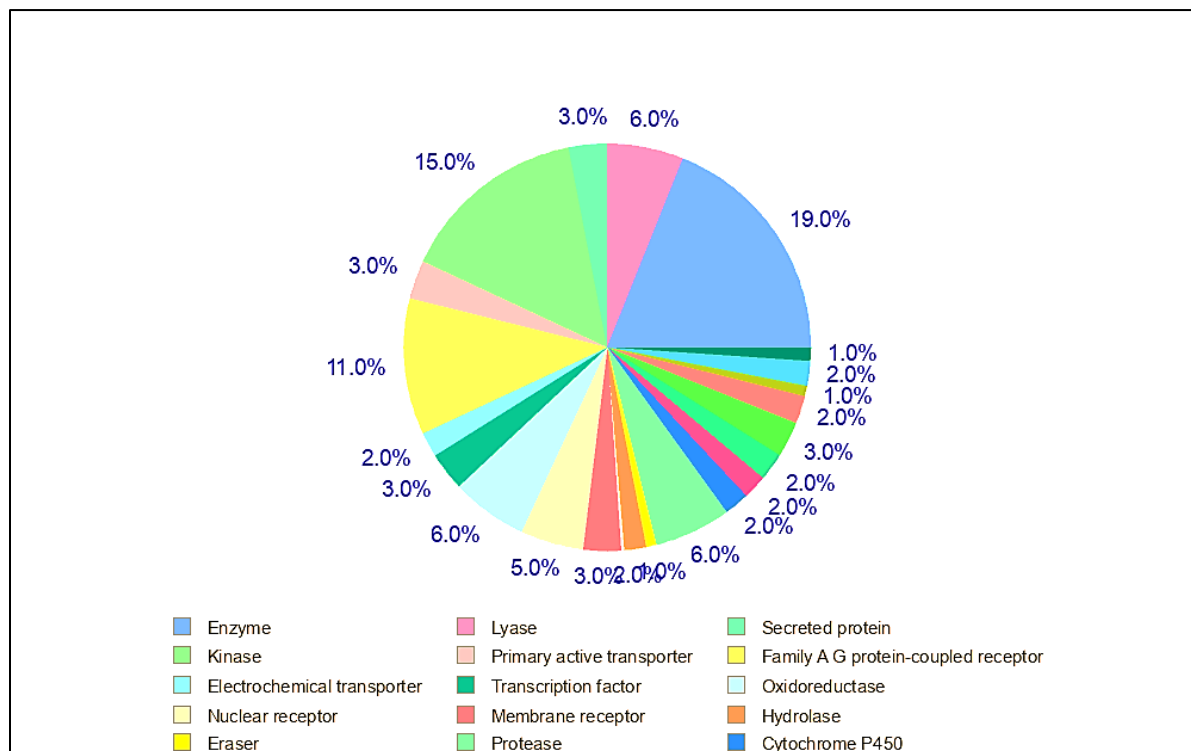


Figure 3.5 Distribution of predicted targets of swertisin in different protein classes by SwissTarget Prediction tool

**Exploring metabolically compromised secretome and bioactives on islet differentiation and function
for effective diabetic therapy**

Gurprit Bhardwaj Ph.D. Thesis 2022

Chapter 3: Identification of molecular targets of Swertisin in glucose homeostasis, islet differentiation & functionality

Target	Common name	Uniprot ID	ChEMBL ID	Target Class	Known actives (3D/2D)
Aldose reductase	AKR1B1	P15121	CHEMBL1900	Enzyme	4 / 69
P-glycoprotein 1	ABCB1	P08183	CHEMBL4302	Primary active transporter	0 / 43
Adenosine A1 receptor (by homology)	ADORA1	P30542	CHEMBL226	Family A G protein-coupled receptor	0 / 17
Protein kinase C (PKC)	PRKCZ	Q05513	CHEMBL3438	Kinase	7 / 0
Arachidonate 5-lipoxygenase	ALOX5	P09917	CHEMBL215	Oxidoreductase	0 / 48
Acetylcholinesterase	ACHE	P22303	CHEMBL220	Hydrolase	0 / 40
Sodium/glucose cotransporter 2	SLC5A2	P31639	CHEMBL3884	Electro chemical transporter	0 / 49
Sigma opioid receptor	SIGMAR1	Q99720	CHEMBL287	Membrane receptor	0 / 51
Dopamine D2 receptor (by homology)	DRD2	P14416	CHEMBL217	Family A G protein-coupled receptor	0 / 46

Table 3.2 Predicted targets of swertisin by SwissTargetPrediction tool

We also performed PASS (Prediction of Activity Spectra for Substances) analysis which also revealed the role of swertisin as a SGLT class inhibitor. PASS is a tool for evaluating the general biological potential of an organic drug-like molecule, which issues concurrent predictions of many types of biological activity based on the structure of compound. PASS analysis is done prior to chemical synthesis and biological testing of a molecule to study and estimate the biological interactions of the molecule (Table 3.3).

Activity	P _a	P _i
Membrane Integrity Agonist	0.957	0.003
Antidiabetic	0.769	0.005
Kinase Inhibitor	0.755	0.009
Cytoprotectant	0.585	0.036
Sodium/Glucose Co-transporter Inhibitor	0.227	0.002
Sodium/Glucose Co-transporter 2 Inhibitor	0.187	0.002
Sodium/Glucose Co-transporter 1 Inhibitor	0.101	0.003

Table 3.3 PASS analysis of swertisin. Activities with $P_a > P_i$ are only considered for a Homology Modelling of hSGLT2 compound. P_a (probability "to be active") calculates the chance that the compound under query resembles the structures of molecules, which are the most typical in a sub-set of "actives" in PASS training set. P_i (probability "to be inactive") calculates the chance that the compound under query resembles the structures of molecules, which are the most typical in a sub-set of "inactives" in PASS training set.

We used computational docking studies to understand structural complexities and binding affinities between the target (SGLT2) and ligand (swertisin). So, we computationally modelled the human SGLT2 structure. The homology model of hSGLT2 constructed using I-TASSER. I-TASSER uses a multi-template threading approach and for construction of the hSGLT2 model, PDB: 3DH4 and PDB: 2XQ2 (Crystal structure of Na/Sugar symporter from *Vibrio parahaemolyticus* were used as major templates.

Chapter 3: Identification of molecular targets of Swertisin in glucose homeostasis, islet differentiation & functionality

Pair-wise sequence Alignment with different variants of SGLT isoforms

A protein BLAST (blastp) was carried out between human SGLT2 structure-3DH4 (Fig 3.6) and hSGLT2-2QX2 (Fig 3.7) was carried out using NCBI-BLAST and the following results were obtained

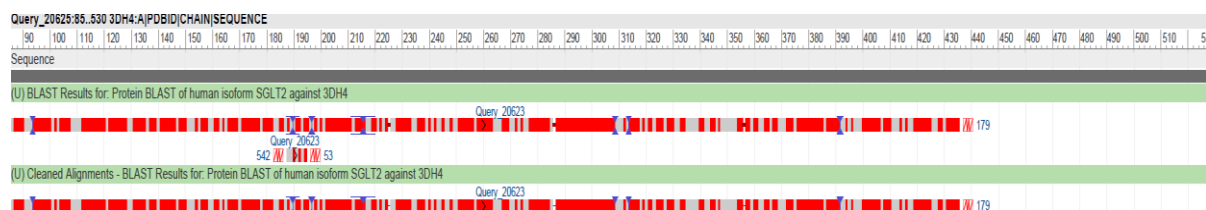


Figure 3.6 Graphical representation of pair-wise alignment of human SGLT2 structure against 3DH4

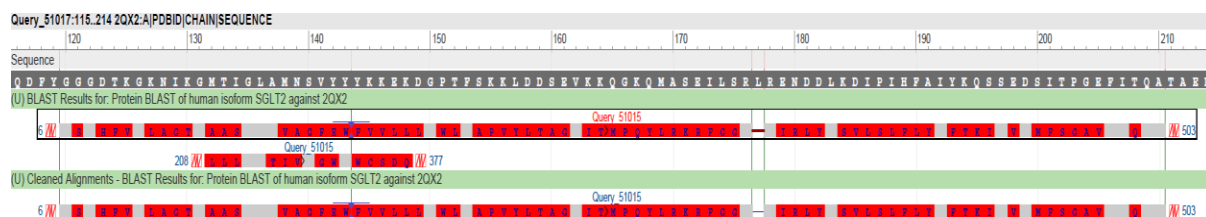


Figure 3.7 Graphical representation of pair-wise alignment of human SGLT2 structure against 2QX2

Description	Max. Score	Total Score	Query-cover	E-Value	Per. Ident
3DH4:hSGLT2	211	227	71%	3e-65	30.75
2QX2:hSGLT2	15.8	30	18%	3.5	23.53

Table 3.4 NCBI-Protein BLAST showing percent identity of human SGLT2 structure against 3DH4 and 2QX2

Chapter 3: Identification of molecular targets of Swertisin in glucose homeostasis, islet differentiation & functionality

Similarly, EMBOSS-pair wise sequence alignment was performed and the following results were obtained

Description	Per. Ident
3DH4:hSGLT2	22.1
2QX2:hSGLT2	24.4

Table 3.5 EMBOSS-pair wise alignment of human SGLT2 structure with 3DH4 and 2QX2

After finding sequence similarity between hSGLT2, 3DH4 and 2QX2 we proceeded with homology modelling of hSGLT2 using I-TASSER. The amino acid sequence of human SGLT2 structure was retrieved from NCBI database (ID: gi4507033). For each target, I-TASSER simulations generate a large ensemble of structural conformations, called decoys. I-TASSER reports up to five models which corresponds to the five largest structure clusters (Table 3.6). The C-score, TM-score and RMSD for the modelled hSGLT2 structure obtained were as follows

Chapter 3: Identification of molecular targets of Swertisin in glucose homeostasis, islet differentiation & functionality


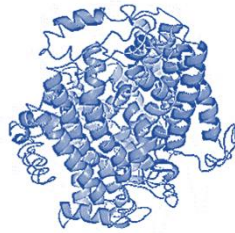
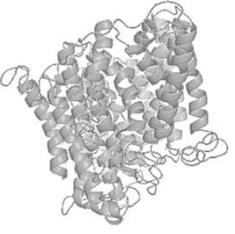


Description	C-score	TM-score	RMSD (estimated)	Structure
Model 1	-0.68	0.63 ± 0.14	$9.6 \pm 4.6 \text{ \AA}$	
Model 2	-1.51	NA*	NA*	
Model 3	-1.61	NA*	NA*	
Model 4	-2.40	NA*	NA*	
Model 5	-2.95	NA*	NA*	

Table 3.6 I-TASSER predicted models of threaded hSGLT2 structures with respective C-scores and TM-scores. *NA: Not available

Chapter 3: Identification of molecular targets of Swertisin in glucose homeostasis, islet differentiation & functionality

Based on the above results, model-1 was used for further simulation studies which was having an acceptable C-score of -0.68 [range: -2 to 5]. The ligand binding site residues of the PDB Hit used for template threading of hSGLT2 by I-TASSER encompassed all the important residues which forms the active site of hSGLT2 (Fig 3.8). Some of the residues are important to be inhibited by a molecule to be placed under SGLT2 inhibitor class.

Rank	C-score	Cluster size	PDB Hit	Lig Name	Download Complex	Ligand Binding Site Residues
1	0.08	4	3dh4A	GAL	Rep. Mult	75,80,98,99,102,286,287,290,291,321,453,457
2	0.08	7	2Q72A	2Q72A06	Rep. Mult	79,82,83,87,157,161,363,444,445,446,448,449,450,451,452,453,454,455
3	0.07	3	3dh4A	NA	Rep. Mult	73,76,389,392,393
4	0.05	4	3F3CA	3F3CA00	Rep. Mult	79,80,154,290,397
5	0.02	2	2WSWA	2WSWA02	Rep. Mult	74,294,295,296,297,396

(a) **C-score** is the confidence score of the prediction. C-score ranges [0-1], where a higher score indicates a more reliable prediction.
 (b) **Cluster size** is the total number of templates in a cluster.
 (c) **Lig Name** is name of possible binding ligand.
 (d) **Rep** is a single complex structure with the most representative ligand in the cluster, i.e., the one listed in the **Lig Name** column.
Mult is the complex structures with all potential binding ligands in the cluster.

Figure 3.8 Figure showing ligand binding site residues of the PDB Hit used for template threading of hSGLT2 by I-TASSER

C. Molecular docking of hSGLT2 with swertisin

Once the human SGLT2 model structure (Fig 3.9) was obtained, it was further evaluated. The model was evaluated by the Ramachandran Plot predicted by the Rampage server (Lovell, Davis et al. 2003). The result analysis showed 92.2% residues in the favoured region, 5.4% residues in the allowed region, and 2.4% residues in the outlier region (Fig 3.10). Swertisin and Canagliflozin also underwent energy minimization. The minimized ligands had final potential energy of 39.62 from initial 90.90 kcal/mol for Swertisin and 20.72 from initial 62.21 kcal/mol for Canagliflozin.

Chapter 3: Identification of molecular targets of Swertisin in glucose homeostasis, islet differentiation & functionality

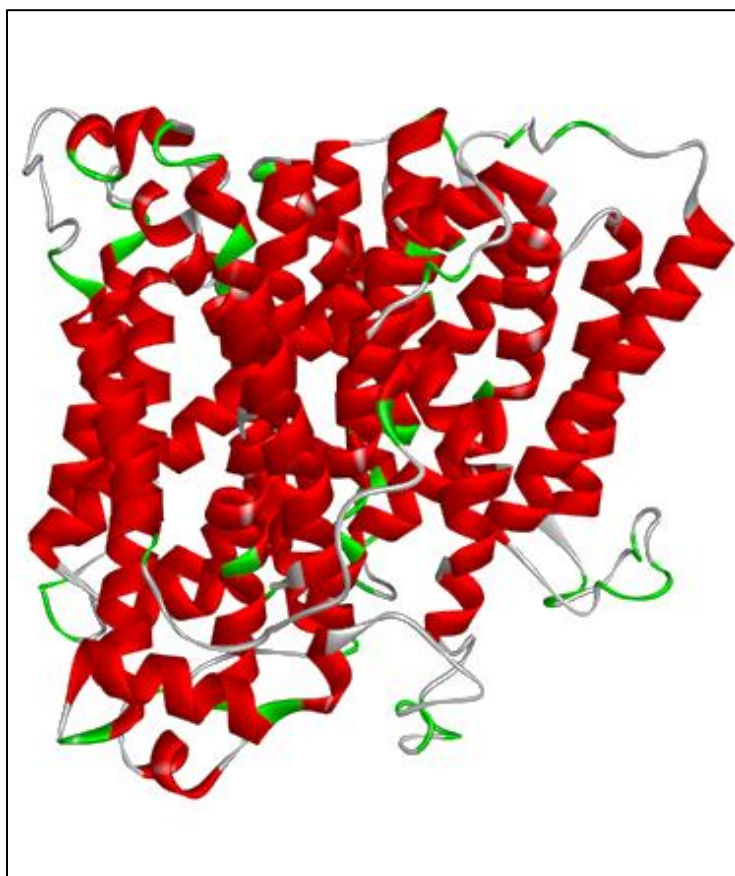


Figure 3.9 Computationally modelled human SGLT2 structure using I-TASSER

Affinity (grid) maps of 15.01 x 21.51 x 18.98 Å grid points with 29.48, -41.04, and 54.97 x, y, and z spacing respectively were generated for molecular docking covering important residues in the active site region. For molecular docking of Swertisin with hSGLT2, SGLT2 inhibitor canagliflozin was also used for docking studies. The docking score for the Swertisin-hSGLT2-interaction and Canagliflozin-hSGLT2-interaction were determined to be -8.5 and -8.7 kcal/mol respectively. In the case of Swertisin, S74, H80, K154, D294, and V296, formed h-bond with C15, O, O1, C10, and O3 atoms of swertisin respectively. The I456 and H80 of hSGLT2 formed a Pi-Alkyl and Pi-Cation interaction with the benzene ring of swertisin respectively (Fig 3.11). Two hydrogen atoms of canagliflozin (H9 & H11) formed hydrogen bonds with T290 and D294, whereas K154 formed an h-bond with S1 atom. H80 of hSGLT2 formed a Pi-Cation interaction with a five-carbon ring of canagliflozin and Pi-Alkyl interaction with C14 atom. The I456 of

Chapter 3: Identification of molecular targets of Swertisin in glucose homeostasis, islet differentiation & functionality

hSGLT2 formed a Pi-Sigma interaction with a benzene ring and Pi-Alkyl interaction with a five-carbon ring of canagliflozin (Fig 3.12). The overall interaction pattern indicates a stable interaction of swertisin within the active binding site of hSGLT2 which is also demonstrated by canagliflozin. Thus *in silico* data gives a similar activity of swertisin with canagliflozin suggesting swertisin a potential candidate for SGLT2 inhibitor.

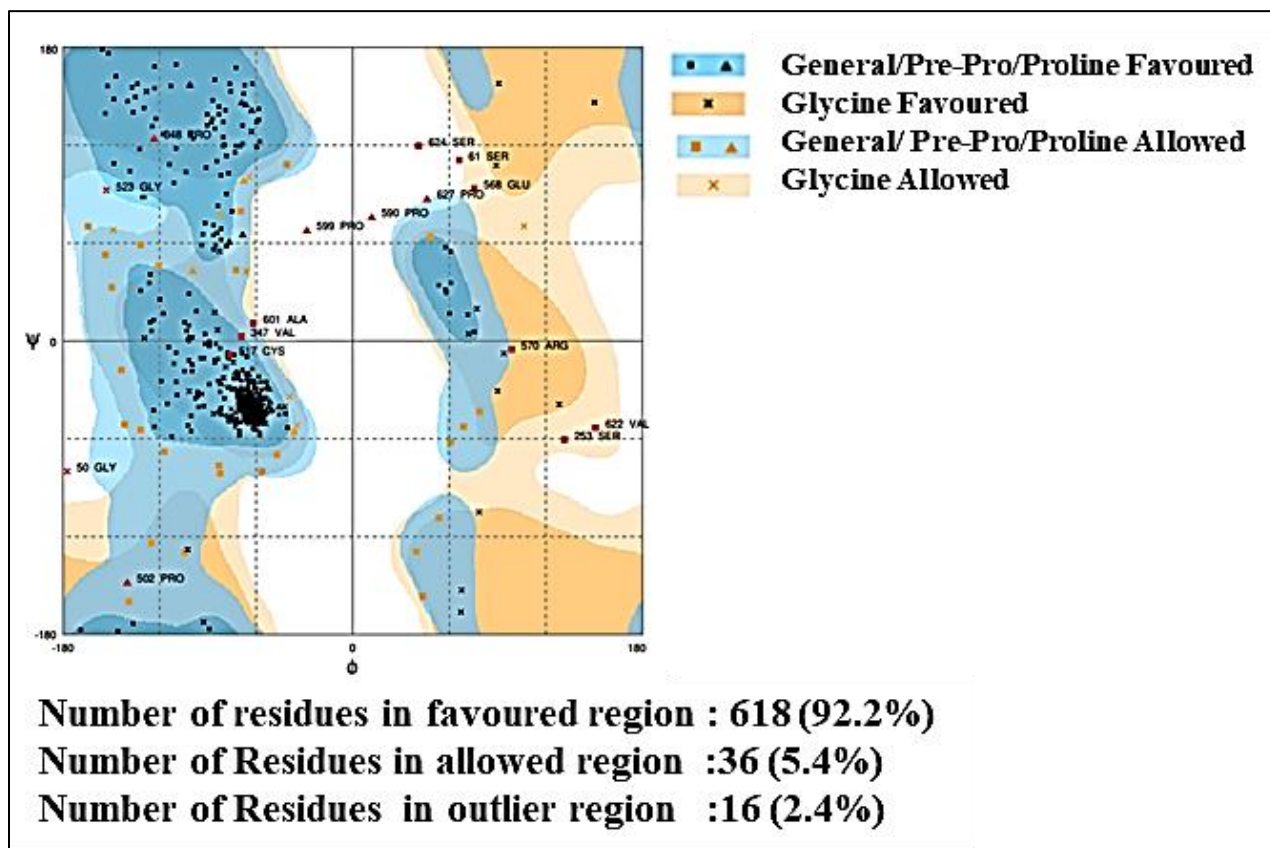


Figure 3.10 Ramchandran plot analysis of modelled human SGLT2 structure

Chapter 3: Identification of molecular targets of Swertisin in glucose homeostasis, islet differentiation &
functionality

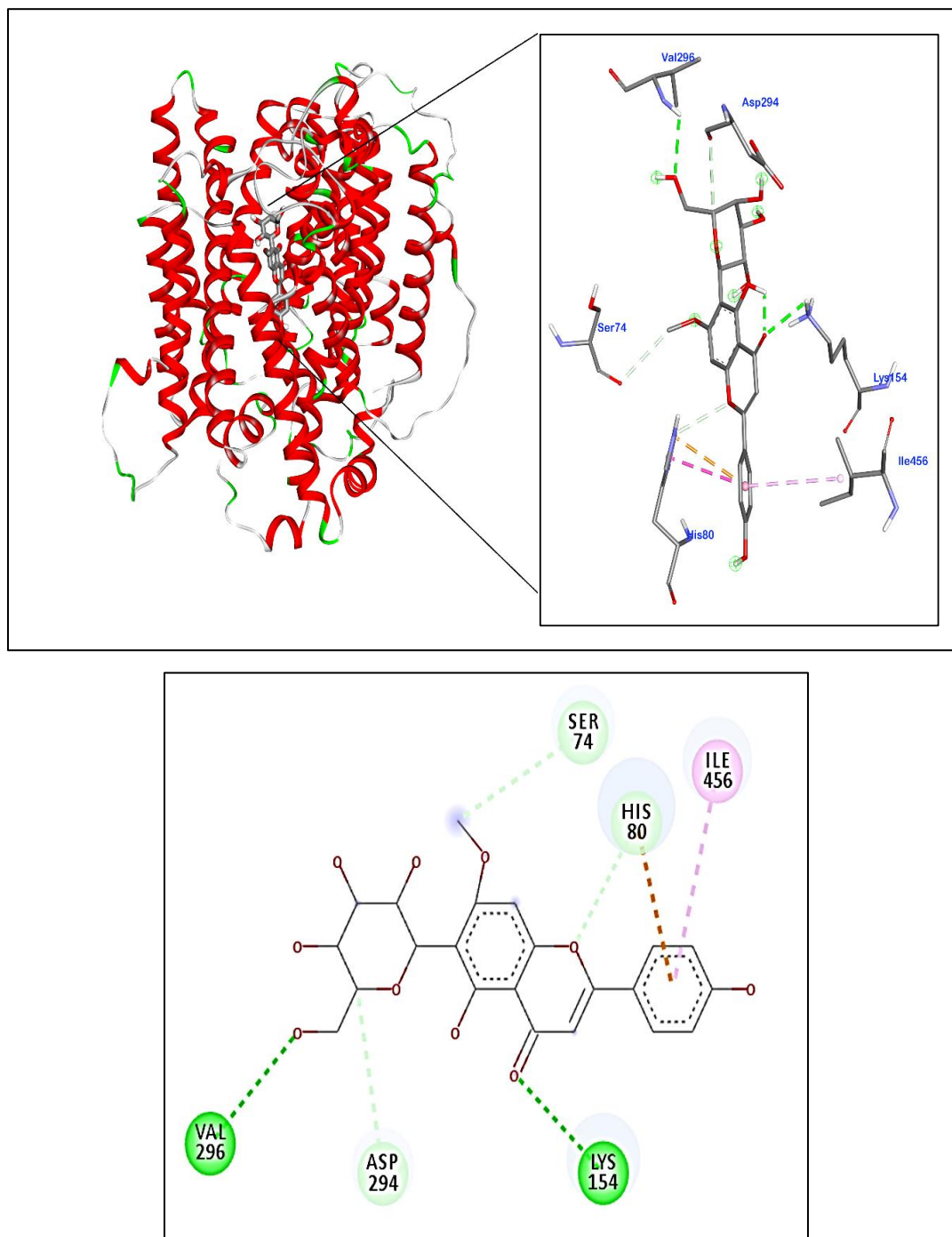


Figure 3.11 Swertisin interacts with key residues within the active site of hSGLT2 by molecular docking. 3D and 2D diagram of molecular docking interaction of Swertisin-hSGLT2

Chapter 3: Identification of molecular targets of Swertisin in glucose homeostasis, islet differentiation &
functionality

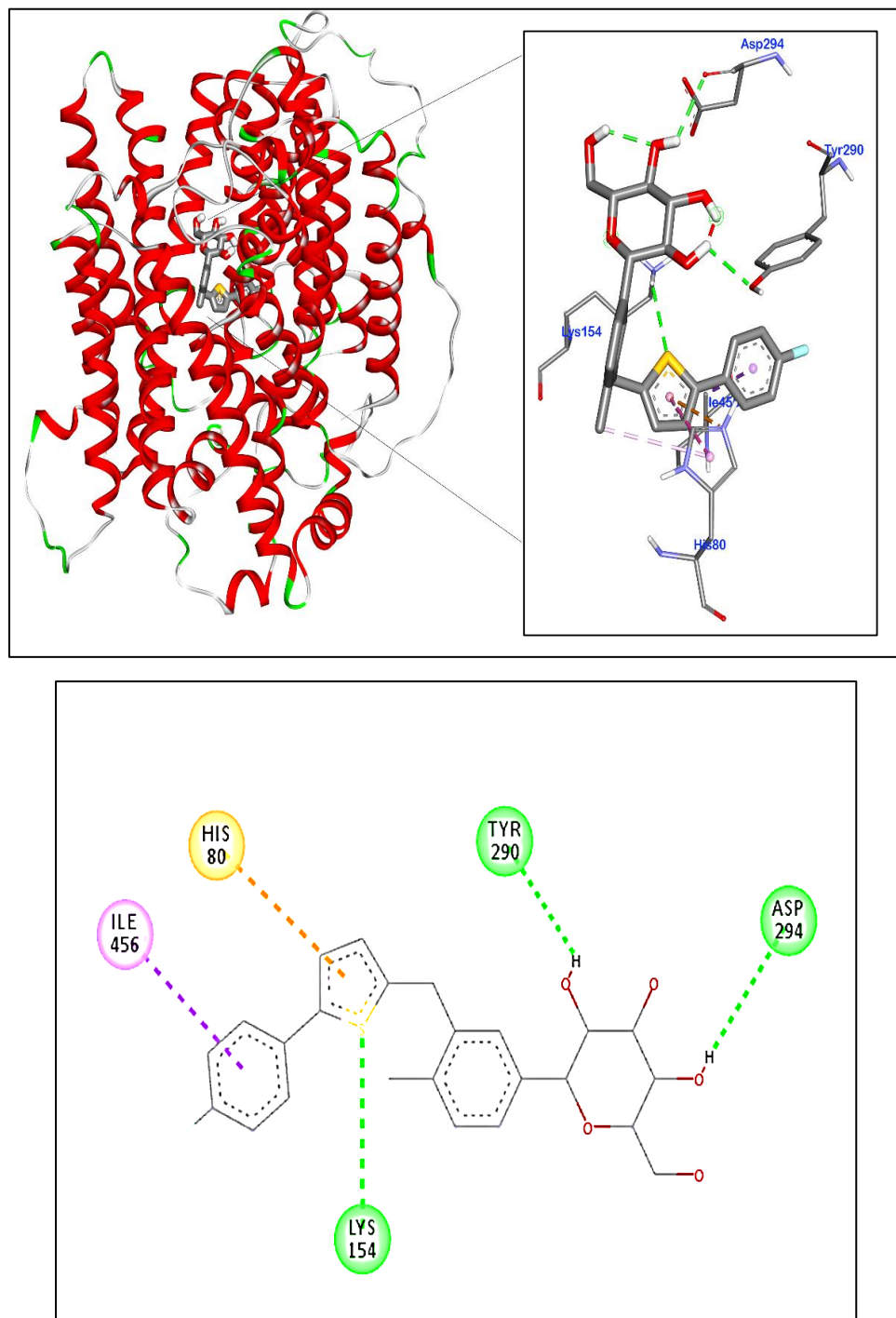


Figure 3.12 3D and 2D diagram of molecular docking interaction of Canagliflozin-hSGLT2

Chapter 3: Identification of molecular targets of Swertisin in glucose homeostasis, islet differentiation & functionality

D. Molecular dynamics simulations

After confirmation of interaction of swertisin in the active site of hSGLT2 by molecular docking, we wanted to study dynamic interactions by molecular dynamic simulations (MDS). A total of three 100 ns MDS (SGLT2; SGLT2-swertisin; and SGLT2-canagliflozin) were carried out to study the stability and conformational dynamics of the protein-inhibitor complexes. The MDS of post-docking complex have been conclusive for deciphering the molecular interaction of the SGLT2-ligand complexes on scales where dynamics of individual atoms are investigated. We analyzed the RMSD, RMSF, H-bonds, as well as PCA properties of the complexes and compared them with apo and reference inhibitor. In addition, the binding free energy of all the complexes was computed for the trajectory retrieved from the last 50 ns.

E. Stability of SGLT2 and SGLT2 with swertisin and canagliflozin

The protein stability of SGLT2 and SGLT2 in complexes with inhibitor were evaluated by RMSD analysis by computing the RMSD values for the C α backbone calculated for the entire 100 ns simulations. RMSD is a means to measure the structural variation between the C α backbones from their initial conformation to their final position during the entire simulation trajectory. Lesser RMSD values indicate higher stability of the simulation. The RMSD values are shown in the plot of RMSD (nm) vs. Time (ns) in Fig 3.13 for SGLT2, SGLT2-canagliflozin, and SGLT2-swertisin. The mean RMSD values for SGLT2, SGLT2-canagliflozin, and SGLT2-swertisin were 0.51 ± 0.044 , 0.51 ± 0.060 and 0.47 ± 0.045 nm, respectively. The overall RMSD comparison of C α backbone showed that the SGLT2-swertisin, was much more stable during the entire simulations compared to apo-protein (SGLT2) and reference inhibitor (SGLT2-canagliflozin).

F. Residue-wise fluctuation and radius of gyration of SGLT2 and SGLT2 with swertisin and canagliflozin

For analysing residue fluctuation during the entire 100 ns MDS, the Root Mean Squared Fluctuations (RMSF) plot was generated. RMSF values of each MDS system were calculated for 100 ns trajectory and overlaid to compare flexible residues in the absence and presence of inhibitor binding (Fig 3.14). The average RMSF value for SGLT2, SGLT2-canagliflozin, and SGLT2-

Chapter 3: Identification of molecular targets of Swertisin in glucose homeostasis, islet differentiation & functionality

swertisin were 0.15 ± 0.099 , 0.16 ± 0.10 , and 0.16 ± 0.099 nm, respectively. Both the SGLT2-canagliflozin and SGLT2-swertisin complexes showed less and similar RMS fluctuations compared to apo-protein, which indicates that inhibitor binding doesn't alter the protein stability and flexibility and hence, these compounds have the potential to bind the SGLT2. The RMSF analysis of the C α protein backbone reveals that the residues around 40-60, 90-100, 260-270, 500-525, 560-570, and 640 showed lesser fluctuations in SGLT2-swertisin when compared with apo-protein (SGLT2) and reference inhibitor (SGLT2-canagliflozin).

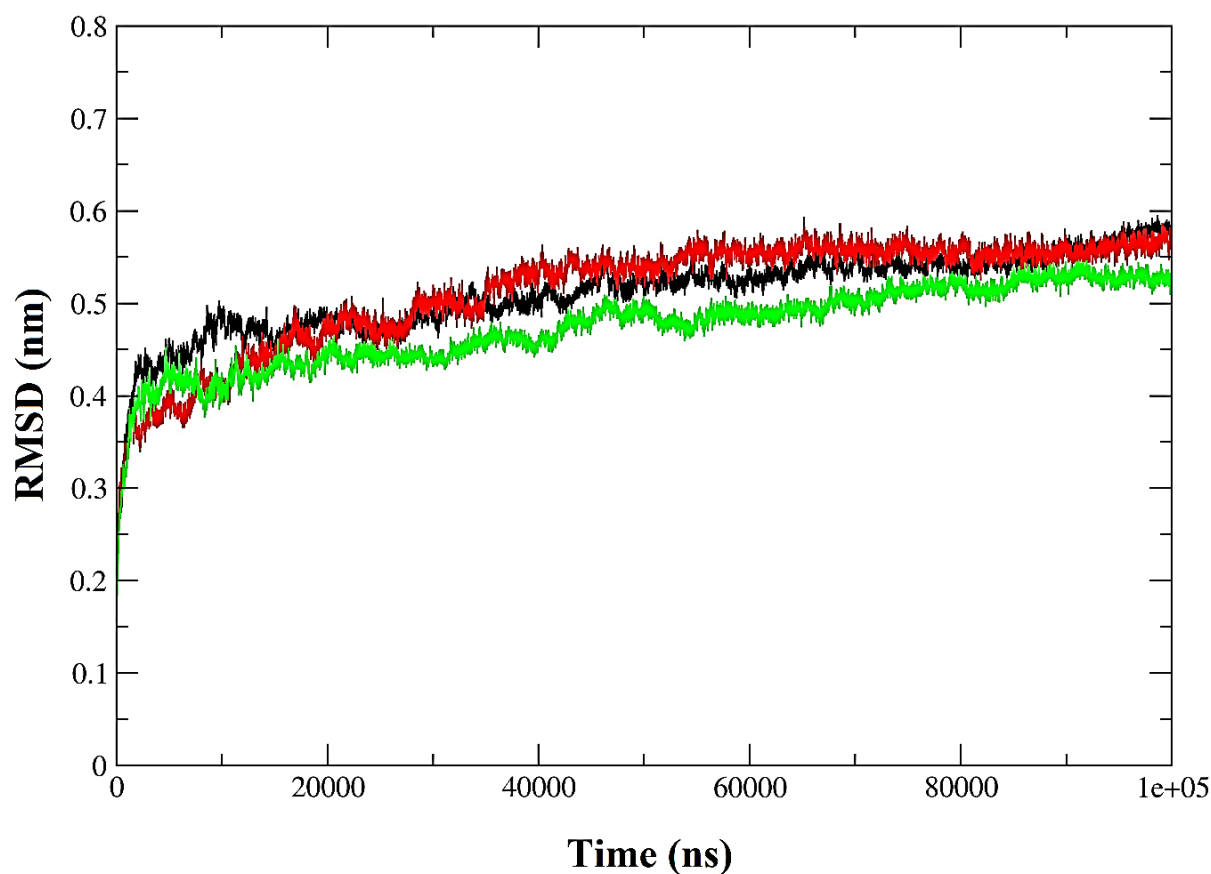


Figure 3.13 Molecular Dynamics Simulations of SGLT2 in apo and inhibitor bound complexes, computing the deviation (nm) versus function of time (100 ns). RMSD of the protein C α backbone atoms of SGLT2 (black), SGLT2-canagliflozin (red), and SGLT2-swertisin (green)

Chapter 3: Identification of molecular targets of Swertisin in glucose homeostasis, islet differentiation &
functionality

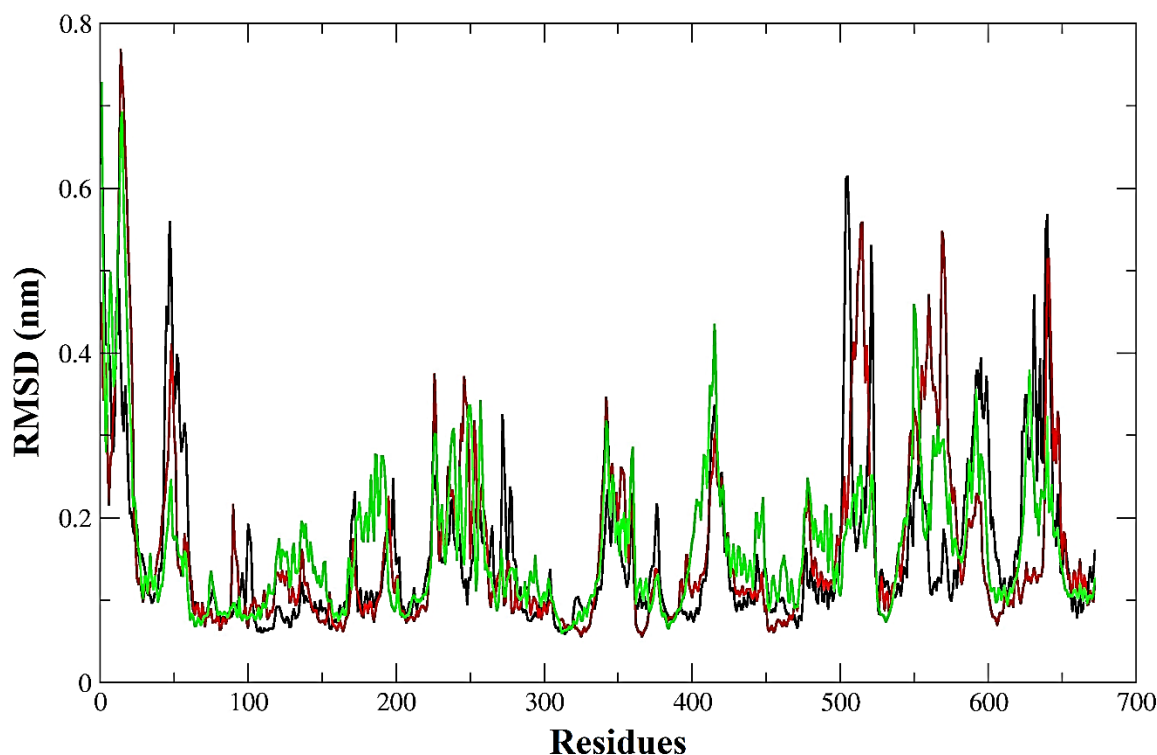


Figure 3.14 Molecular Dynamics Simulations of SGLT2 in apo and inhibitor bound complexes, computing the residue-wise RMSF deviations (nm). RMSF deviation plot of the protein Ca backbone atoms of SGLT2 (black), SGLT2-canagliflozin (red), and SGLT2-swertisin (green)

Among the easier techniques to evaluate the stability of a protein throughout an MD, simulation is to compute the radius of gyration, (R_g) which is a criterion that explains the stable conformation of a system. In this study, the average R_g values of SGLT2, SGLT2-canagliflozin, and SGLT2-swertisin were 2.41 ± 0.023 , 2.39 ± 0.027 , and 2.39 ± 0.025 nm, respectively. The R_g of SGLT2, SGLT2-canagliflozin and SGLT2-swertisin shows a minor difference (Fig 3.15), which shows that the binding of ligands did not affect the compactness of the protein. Indeed compared to SGLT2, SGLT2-canagliflozin and SGLT2-swertisin showed a lesser deviation in SGLT2.

Chapter 3: Identification of molecular targets of Swertisin in glucose homeostasis, islet differentiation & functionality

G. Molecular interaction through hydrogen bonding.

The Hydrogen bond formation (H-bond) is the key determinants of specificity and molecular interactions between protein and inhibitor molecule. The average H-bonds formed within protein and protein and ligand were calculated for entire 100 ns MDS trajectories and are plotted in Fig 3.16a and b . The average number of intra H-bonds formed in the entire production MDS for SGLT2, SGLT2-canagliflozin and SGLT2-swertisin were 474.27 ± 12.10 , 491.71 ± 19.12 and 483.92 ± 16.19 respectively. Overall, the number of intra-bonds were similar showing no significant change in SGLT2 upon binding with canagliflozin and swertisin. The average number of H-bonds formed between protein and ligand in the entire production MDS for SGLT2-canagliflozin and SGLT2-swertisin were 1.27 ± 1.01 and 1.36 ± 1.06 respectively.

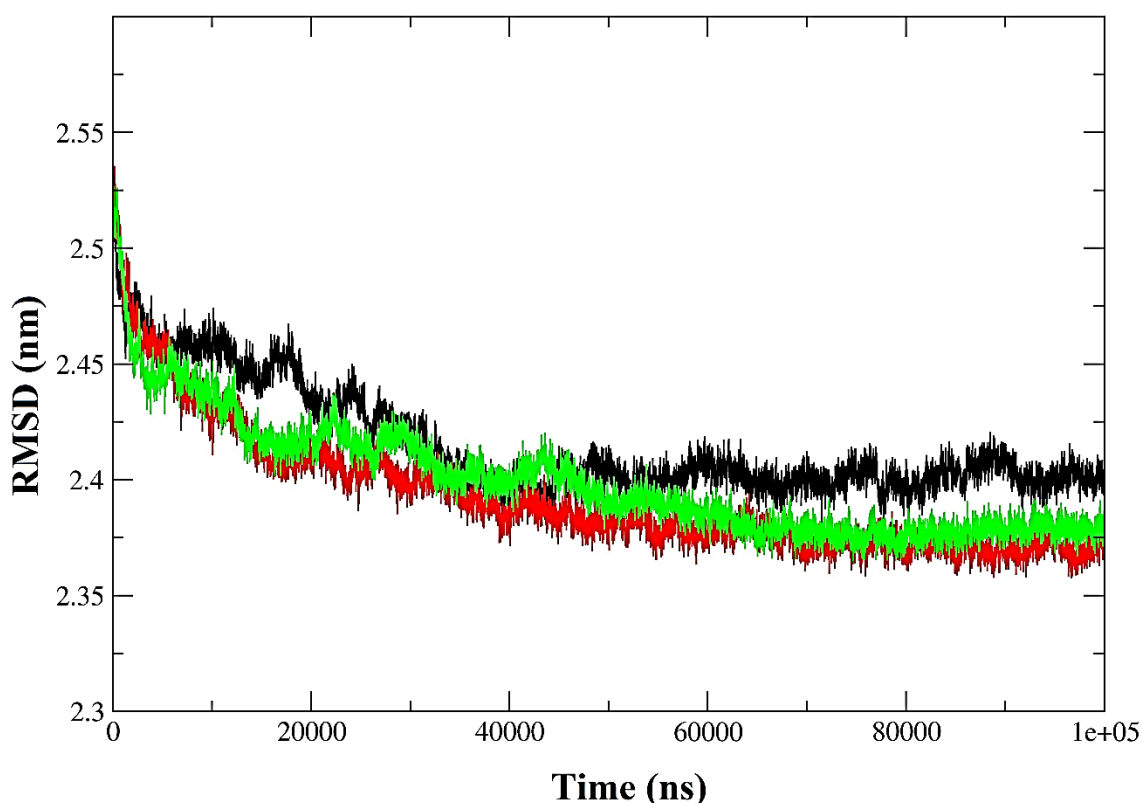


Figure 3.15 Molecular Dynamics Simulations of SGLT2 in apo and inhibitor bound complexes, computing the radius of gyration (nm) versus function of time (100 ns). RoG of

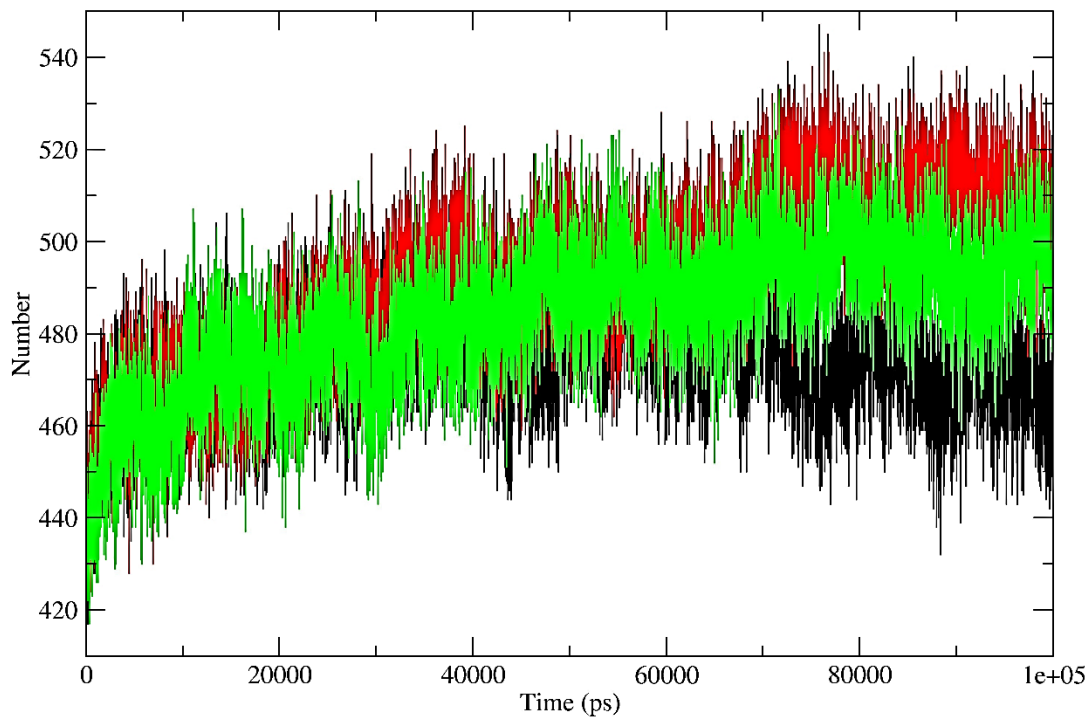
Chapter 3: Identification of molecular targets of Swertisin in glucose homeostasis, islet differentiation & functionality

the protein Ca backbone atoms of SGLT2 (black), SGLT2-canagliflozin (red), and SGLT2-swertisin (green)

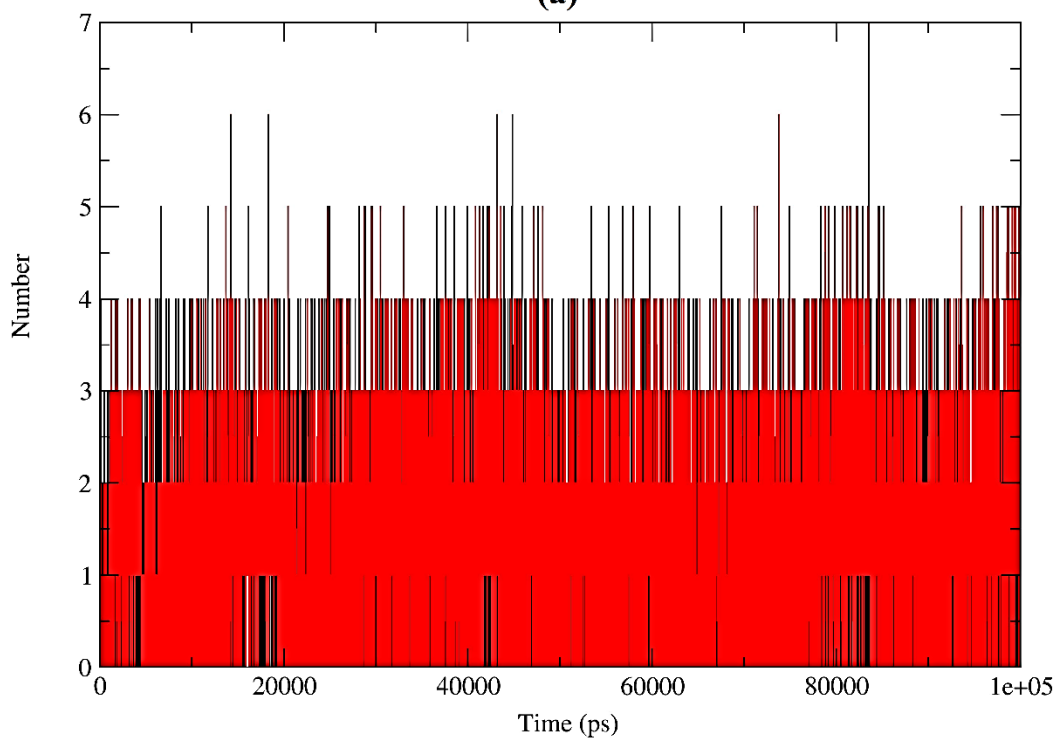
H. Difference in interactions network of SGLT2 and SGLT2 with swertisin and canagliflozin complexes through dynamics cross-correlation matrix (DCCM):

Hydrogen bond interactions were correlated with dynamics cross-correlation matrix, where the interaction between SGLT2 with respect to canagliflozin and swertisin were calculated throughout the trajectory of 100 ns. As shown in Fig 3.17, Dynamics cross-correlation matrix was calculated between proteins motions in both apo and protein complexes. It is feasible to compute the dynamic correlation between all atoms inside the molecule, or the degree to which they move together, by examining the system's trajectories. The 2D diagrams of DCCM showed the correlated motions between residues during the whole simulation process. DCCM showed the overall correlation, which ranged from -1.0 to 1.0 (from magenta to cyan). Different colors were used to define different degrees of correlation between residues, and the darker the color, the stronger the correlation. The positive correlation (from 0.25 to 1) meant that the residues moved in the same direction, while the negative correlation (from -1 to 0.25) meant that the residues moved in the opposite direction. While white color indicates no cross-correlation. From DCCM it is clearly evident that residue interaction in SGLT2 was similar with that found with SGLT2-swertisin. The reference inhibitor canagliflozin DCCM values were very different when compared to SGLT2 and SGLT2-swertisin.

Chapter 3: Identification of molecular targets of Swertisin in glucose homeostasis, islet differentiation &
functionality



(a)



(b)

Chapter 3: Identification of molecular targets of Swertisin in glucose homeostasis, islet differentiation & functionality

Figure 3.16 Intra and Inter hydrogen bonds of SGLT2 in apo and inhibitor bound complexes: (a) Intra H-bond formation plot computed versus function of time (100 ns) between protein and inhibitor in SGLT2 (black), SGLT2-canagliflozin (red), and SGLT2-swertisin (green). (b) Number of hydrogen bonds computed versus function of time (100 ns) between SGLT2 and inhibitor in SGLT2 (black), SGLT2-canagliflozin (red), and SGLT2-swertisin (green)

The H-bond occupancy of protein atoms with inhibitor atoms were computed and summarize as below in Table 3.7.

Canagliflozin			Swertisin		
Found 26 hbonds.			Found 26 hbonds.		
donor	acceptor	occupancy	donor	acceptor	occupancy
CAN673-Side	SER74-Main	0.08%	SER400-Side	SWR673-Side	0.01%
SER460-Side	CAN673-Side	28.78%	SWR673-Side	SER74-Side	0.01%
LYS154-Side	CAN673-Side	0.03%	SER161-Side	SWR673-Side	0.01%
SER74-Side	CAN673-Side	0.06%	SWR673-Side	GLN295-Side	0.42%
GLY79-Main	CAN673-Side	1.91%	GLN295-Side	SWR673-Side	0.01%
SER161-Side	CAN673-Side	0.02%	TRP289-Side	SWR673-Side	2.12%
GLN295-Side	CAN673-Side	1.36%	LYS154-Side	SWR673-Side	3.95%
CAN673-Side	SER78-Side	0.16%	SWR673-Side	PHE453-Side	0.13%
CAN673-Side	GLN295-Side	0.07%	SWR673-Side	SER393-Main	0.32%
CAN673-Side	TYR290-Side	0.04%	VAL296-Main	SWR673-Side	0.40%
CAN673-Side	SER393-Side	0.09%	SWR673-Side	ASP294-Main	1.38%
CAN673-Side	SER78-Main	0.11%	SWR673-Side	SER396-Side	0.56%
CAN673-Side	ALA389-Main	0.54%	SWR673-Side	SER74-Main	0.42%

Chapter 3: Identification of molecular targets of Swertisin in glucose homeostasis, islet differentiation & functionality

CAN673-Side	HIS80-Side	0.17%	SER393-Side	SWR673-Side	0.36%
THR153-Side	CAN673-Side	0.61%	SWR673-Side	TYR290-Main	0.08%
CAN673-Side	GLY77-Main	0.23%	SWR673-Side	ASN75-Side	0.14%
HIS80-Main	CAN673-Side	0.24%	SER396-Side	SWR673-Side	0.04%
SER78-Main	CAN673-Side	0.08%	SWR673-Side	SER393-Side	0.13%
CAN673-Side	SER74-Side	0.42%	SWR673-Side	TRP289-Main	0.03%
SER393-Side	CAN673-Side	0.05%	SWR673-Side	GLN295-Main	0.02%
CAN673-Side	SER392-Side	0.16%	ASN75-Side	SWR673-Side	0.01%
CAN673-Side	ILE76-Main	0.48%	SWR673-Side	GLY79-Main	0.01%
CAN673-Side	GLY79-Main	0.07%	TYR290-Side	SWR673-Side	0.01%
CAN673-Side	LEU390-Main	0.04%	SWR673-Side	ILE397-Side	0.01%
CAN673-Side	ASN75-Main	0.04%	SWR673-Side	GLY83-Main	0.01%
SER393-Main	CAN673-Side	0.01%	SWR673-Side	TYR290-Side	0.01%

Table 3.7 Summary of H-bond occupancy between SGLT2 and SGLT2 complexes with canagliflozin and swertisin

I. Principal Component Analysis (PCA)

The principal component analysis predicts the associated motion of complexes, and the overall movements in the proteins are represented by a few essential eigenvectors in the computation of the Principal Components (PCs). It computes the covariance matrix of positional changes for C-alpha atoms to interpret the dynamics of SGLT2 and SGLT2-inhibitor interactions. All through the x and y-axis signifies the one conformation of the protein. The spread out of blue and red dots defined the level of conformational adjustments in simulation, where shade range develop from blue to white to red is comparable to simulation time. The blue demonstrates starting time step, white is moderate and the last time step is addressed by red. The unsteady conformation state (displayed in blue) can be quickly divided in neared convergence to acquire a steady conformational specify (displayed in red). The eigenvectors indicate the direction of the motion of

Chapter 3: Identification of molecular targets of Swertisin in glucose homeostasis, islet differentiation & functionality

atoms while the eigenvalues represent the magnitude of the motion. To measure the effectiveness of the canagliflozin and swertisin on the conformational state of SGLT2 protein, the MD simulation trajectories were used to perform the PCA of C α atoms of all three MDS. The Eigenvalues for the SGLT2, SGLT2-canagliflozin and SGLT2-swertisin are 23.3, 22.5 and 35 respectively as shown in Fig 3.18. The complexes with a steep drop in Eigen fraction correspond to the early five eigen modes and represent ~% displacement in the residual motion of the protein; these results represent the significant induced conformation fluctuations in the SGLT2 due to suitable inhibitor interaction in the cavity. The eigen data for SGLT2-swertisin had a steep deep indicating early stable complex formation compared to SGLT2-canagliflozin.

J. Binding free energy estimation and energy decomposition of SGLT2 complexes with canagliflozin and swertisin:

The binding free energy (ΔG) between SGLT2-inhibitor complexes was calculated using the MM-PBSA method for the 50 ns stable trajectories. The MM-PBSA method for computing binding free energy is based on MD simulations of the SGLT2-inhibitor complex and are therefore intermediate in both accuracy and computational effort between empirical scoring and alchemical perturbation methods. A total of 200 frames at every 250 ps from 50 ns trajectories were chosen for ΔG calculation which is an overall estimate of the converged non-bonded interaction energies. The ΔG values for SGLT2, SGLT2-canagliflozin, and SGLT2-swertisin were negative (Fig 3.19). The individual component for binding energy, the Van der Waals, the electrostatic interactions and non-polar solvation energy had contributed negatively to the overall interaction energy. To gain more insights into key residues involved in ligand binding, the residue-wise energy decomposition plot was generated which shows the total binding energy contribution for each residue for all three MDS.

Chapter 3: Identification of molecular targets of Swertisin in glucose homeostasis, islet differentiation &
functionality

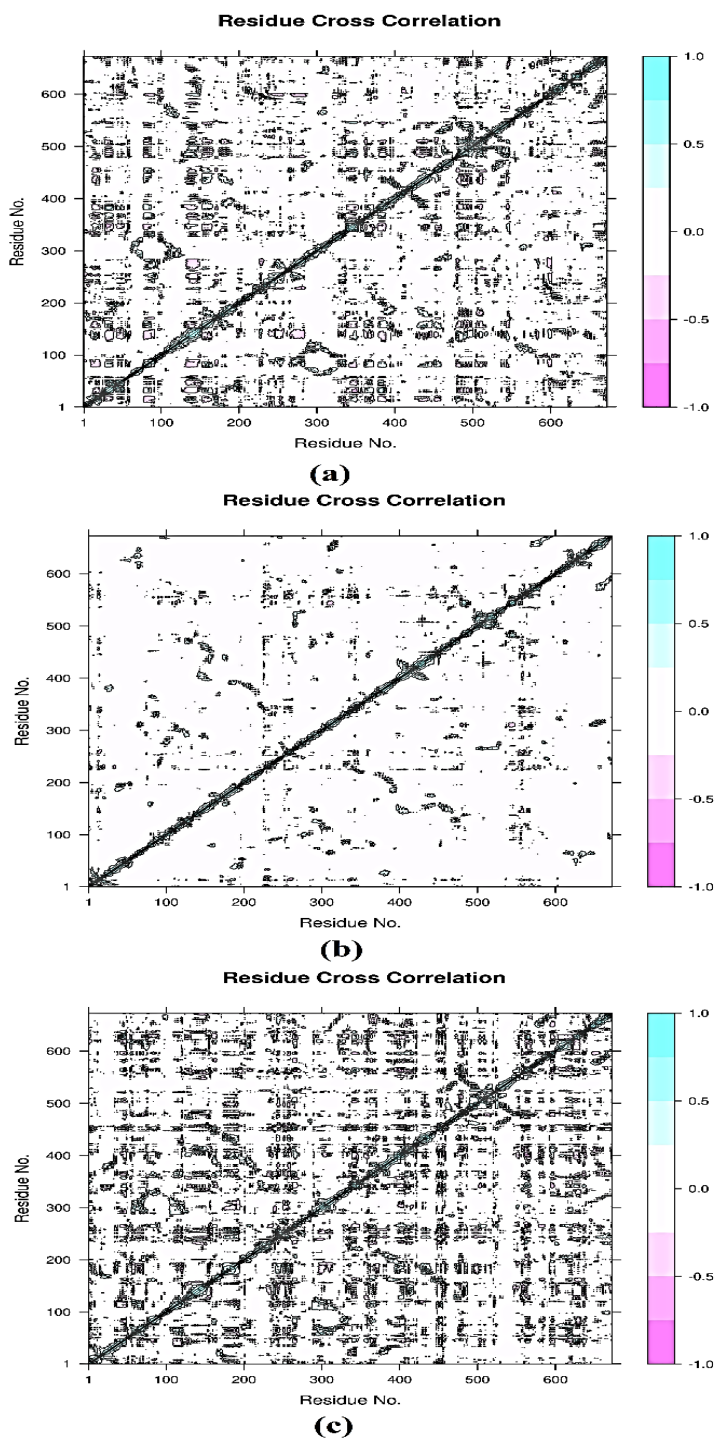


Figure 3.17 Dynamics cross-correlation for SGLT2, SGLT2-canagliflozin and SGLT2-swertisin complexes. DCCM was calculated according to time average of Ca atoms. The

Chapter 3: Identification of molecular targets of Swertisin in glucose homeostasis, islet differentiation & functionality

whole range of correlation from -1 to $+1$ is represented in three ranges: cyan color corresponding to positive correlation values ranging from 0.25 to 1 ; magenta color corresponding to negative correlation values ranging from -0.25 to -1 ; and white color corresponding to weak or no-correlation values ranging from -0.25 to $+0.25$. The extent of correlation or anti-correlation is indicated by variation in the intensity of respective cyan or magenta color in SGLT2 (a), SGLT2-canagliflozin (b), and SGLT2-swertisin (c)

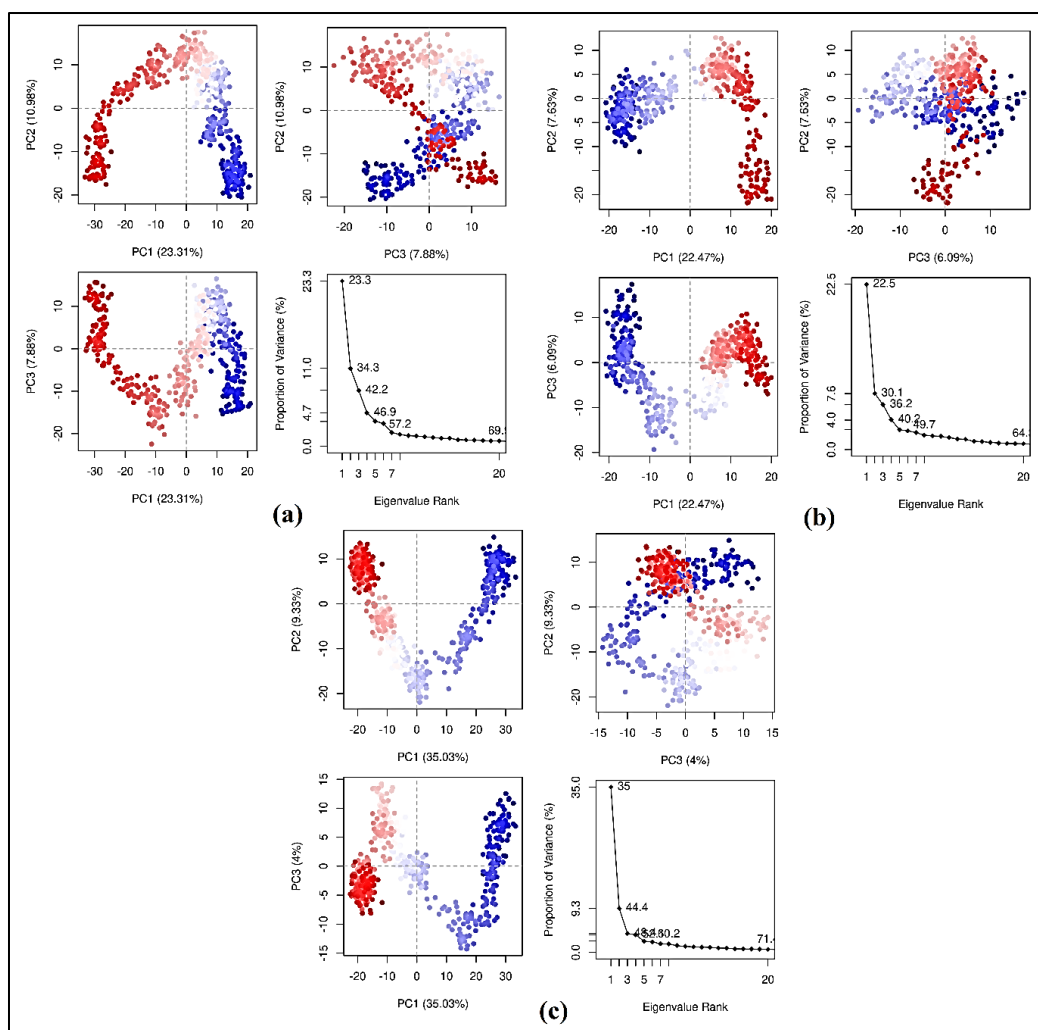


Figure 3.18 PCA analysis for SGLT2 (a), SGLT2-canagliflozin (b), and SGLT2-swertisin (c). In all three sections, the PC1, PC2 and PC3 eigen values are plotted against each other and the fourth section indicates the plot of population variance and eigenvalue rank

Chapter 3: Identification of molecular targets of Swertisin in glucose homeostasis, islet differentiation &
functionality

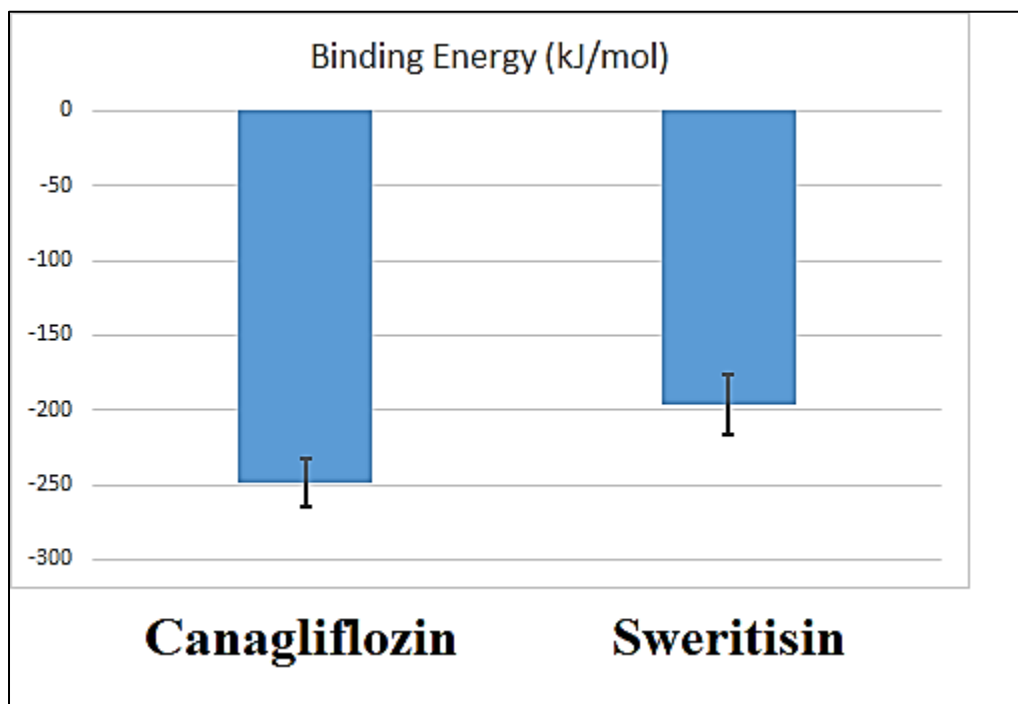


Figure 3.19 MM-PBSA Calculation for binding free energy. The total binding free energy for all the SGLT2-inhibitor complexes calculated for last 50 ns stable trajectory for a total of 200 frames, each at 250 ps interval

3.3.2 *In vitro* molecular target identification of swertisin for glucose lowering effect

A. Swertisin suppresses sodium dependent glucose uptake by selectively inhibiting SGLT2

SGLT2 and GLUT2 are major glucose transporters present in the kidney which facilitates glucose reabsorption in the blood which is sodium dependent and independent respectively (Ghezzi, Loo et al. 2018). Since the computational analysis affirmed the interaction of swertisin to that of SGLT2 which is mainly expressed in the kidney; *in vitro* investigation was performed to assess the sodium dependent and independent 2-NBDG uptake by swertisin in the HEK293 cell line. To probe whether swertisin interacts with GLUT transporter, uptake was performed in sodium free buffer. SGLT2 dependent uptake was again followed by sodium buffer with cytochalasin B respectively. Cytochalasin B is well characterized for inhibition of glucose transport by GLUTs (Kapoor, Finer-

Chapter 3: Identification of molecular targets of Swertisin in glucose homeostasis, islet differentiation & functionality

Moore et al. 2016) (Ebsten and Plagemann 1972). It inhibited 2-NBDG uptake in pancreatic (Yamada, Saito et al. 2007) and endothelial cells (Blodgett, Kothinti et al. 2011). Some biochemical studies have demonstrated that cytochalasin B binds at or near to the sugar export site of GLUT1 in RBCs (Sergeant and Kim 1985).

These tests revealed that 7.5 $\mu\text{g/ml}$ concentration of swertisin strongly inhibited sodium dependent glucose uptake, reducing 2-NBDG from 100% to 51.4% and 30.4% in the absence or presence of cytochalasin B respectively compared to control. Uptake inhibition was consistent even at higher concentrations of swertisin. Whereas canagliflozin demonstrated reduced 2-NBDG by 34.36 % from 100 % at 13 $\mu\text{g/ml}$ in sodium buffer with cytochalasin B compared to control. These results point out almost similar degree of glucose uptake inhibition by swertisin at a much lower dose than canagliflozin. As anticipated our sodium independent uptake of 2-NBDG experiment demonstrated that it was unaffected by swertisin (Fig 3.20).

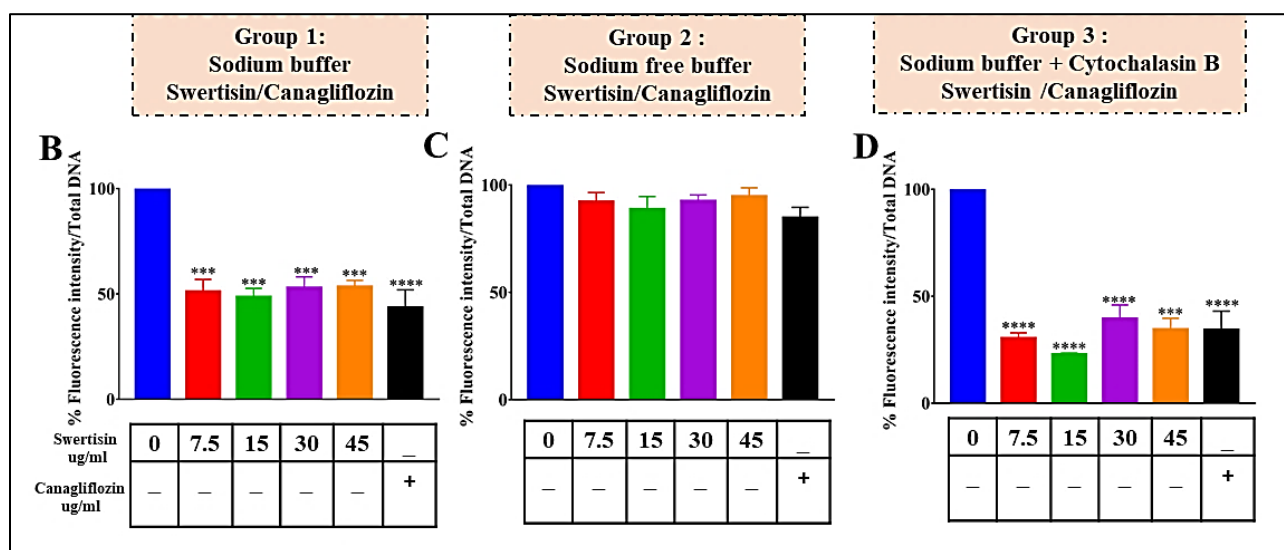


Figure 3.20 SGLT2 specific inhibition by swertisin affects sodium dependent glucose uptake *in vitro* in HEK293 cell line. Sodium dependent glucose uptake assay was performed in the HEK293 cell line. Swertisin treatment was given at varying doses and uptake inhibition of 2-NBDG was performed in (B) sodium buffer (C) sodium free buffer and (D) sodium buffer with 10 μM cytochalasin B (GLUT inhibitor) for 60 min. Canagliflozin was taken as a

Chapter 3: Identification of molecular targets of Swertisin in glucose homeostasis, islet differentiation & functionality

positive control. Results are represented as % Fluorescence intensity per total DNA \pm SEM, N=3. Significance is expressed as p-value * <0.001, **** <0.0001 control vs treatment groups. G=Glucose, S=Swertisin, C=Cytochalasin B**

Further, fluorescence microscopy analysis demonstrated time-dependent intracellular accumulation of 2-NBDG in HEK293 cells in control where it preferentially localizes inside the cell. Whereas striking aggregation of 2-NBDG on HEK293 cell membrane in swertisin treated cells was evident where 2-NBDG can be observed as confined to the HEK293 cell membrane. These results further strengthen our conviction about the SGLT2 inhibition property of swertisin (Fig 3.21).

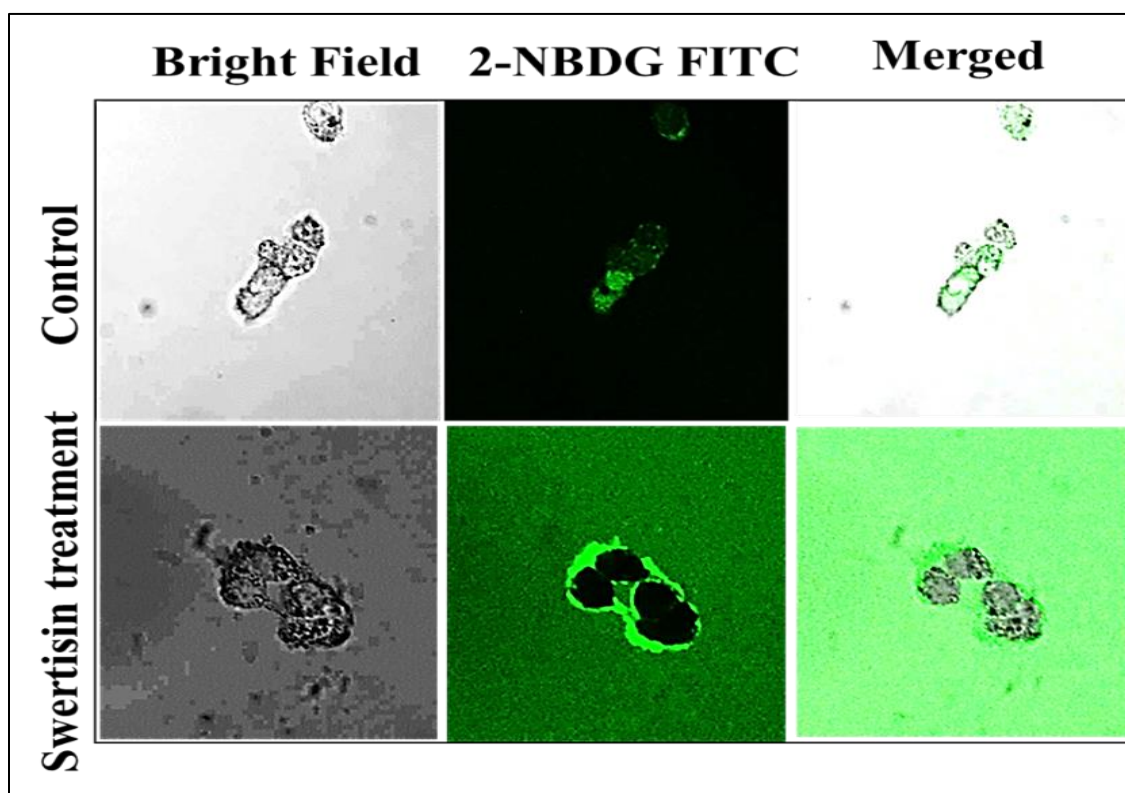


Figure 3.21 Representative time dependent fluorescence imaging of uptake was performed. HEK293 cells were incubated in sodium buffer in the absence (Control) and presence of 7.5 μ g/ml swertisin with 10 μ M cytochalasin B for 10 min in presence of 2-NBDG (green) (Magnification:20X).

Chapter 3: Identification of molecular targets of Swertisin in glucose homeostasis, islet differentiation & functionality

To study the effect of swertisin on SGLT1, we performed similar sodium dependent and independent 2-NBDG uptake in Caco2 cell line. We observed unaltered and non-significant inhibition of glucose uptake even at a higher concentration of swertisin. Thus, swertisin displayed higher selectivity of SGLT2 rather than SGLT1 at lower inhibitory concentration compared to canagliflozin (Fig 3.22).

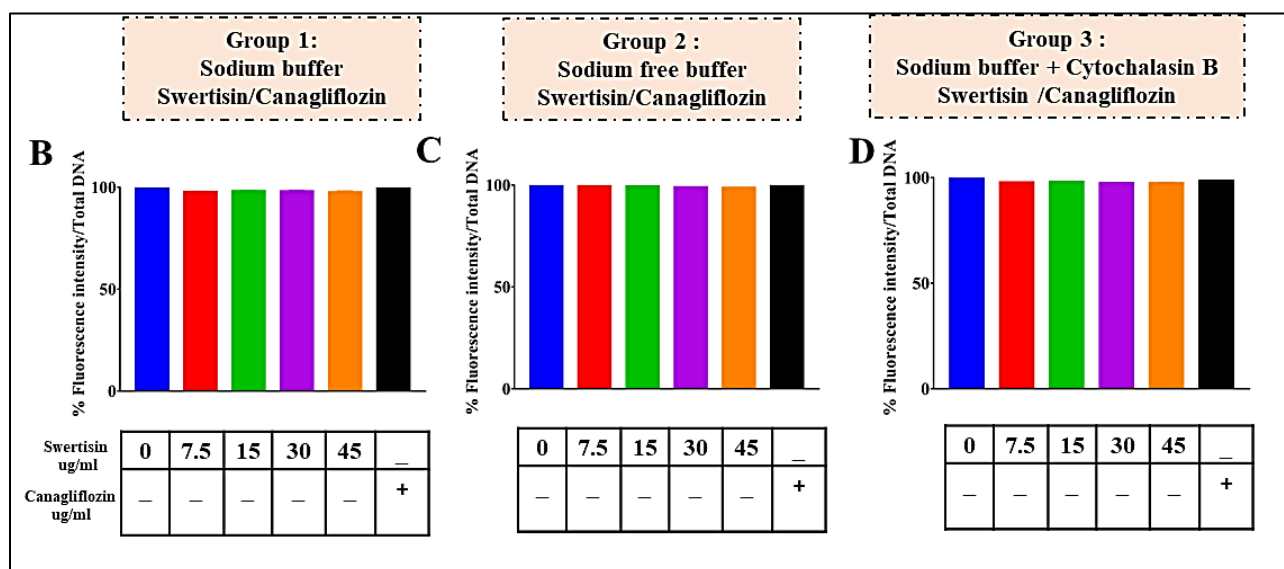


Figure 3.22 Sodium dependent glucose uptake demonstrating unaltered SGLT1 inhibition by swertisin. Sodium dependent glucose uptake assay was performed in the Caco2 cell line. Swertisin treatment was given at varying doses and uptake inhibition of 2-NBDG was performed in (B) sodium buffer (C) sodium free buffer and (D) sodium buffer with 10 μ M cytochalasin B (GLUT inhibitor) for 60 min. Canagliflozin was taken as a positive control. Results are represented as % Fluorescence intensity per total DNA \pm SEM, N=3. G=Glucose, S=Swertisin, C=Cytochalasin B

B. Swertisin regulates key SGLT2 related proteins

One of the contributing factors in uptake of glucose by the transporters in the cells depends on the expression of the transporter protein which in turn is regulated by many factors. So we wanted to determine whether swertisin contributed to the regulation of SGLT2 expression, we examined the time-dependent expression of SGLT2 in presence of swertisin. As expected, incubation of the

Chapter 3: Identification of molecular targets of Swertisin in glucose homeostasis, islet differentiation &
functionality

HEK293 cell line with 7.5 µg/ml swertisin abolished the induction of SGLT2 expression in a time dependent manner. Evident downregulation of SGLT2 protein expression was persisted till 12 H incubation with swertisin compared to control.

It led us to explore the protein expression of kinases which contributes to the regulation of SGLT2. Stimulation of Protein kinase C is known to regulate SGLT2. pp38 MAPK and Erk1/2 also plays role in regulating the expression of the SGLT2 (Haneda, Araki et al. 1997, Lee, Lee et al. 2007) In the present study, we observed downregulation of SGLT2 with the upregulation of PKC from 4H till 12H of post swertisin treatment incubation.

SGLT2 regulation by PKC involves pp38 MAPK which also demonstrated increased expression than control at 12H. Another important kinase is ERK1/2 and non-significant change was observed until 12H. Thus, temporal analysis of SGLT2 levels with swertisin treatment demonstrated overall downregulation of SGLT2 with differential regulation of regulating proteins (Fig 3.23).

Chapter 3: Identification of molecular targets of Swertisin in glucose homeostasis, islet differentiation & functionality

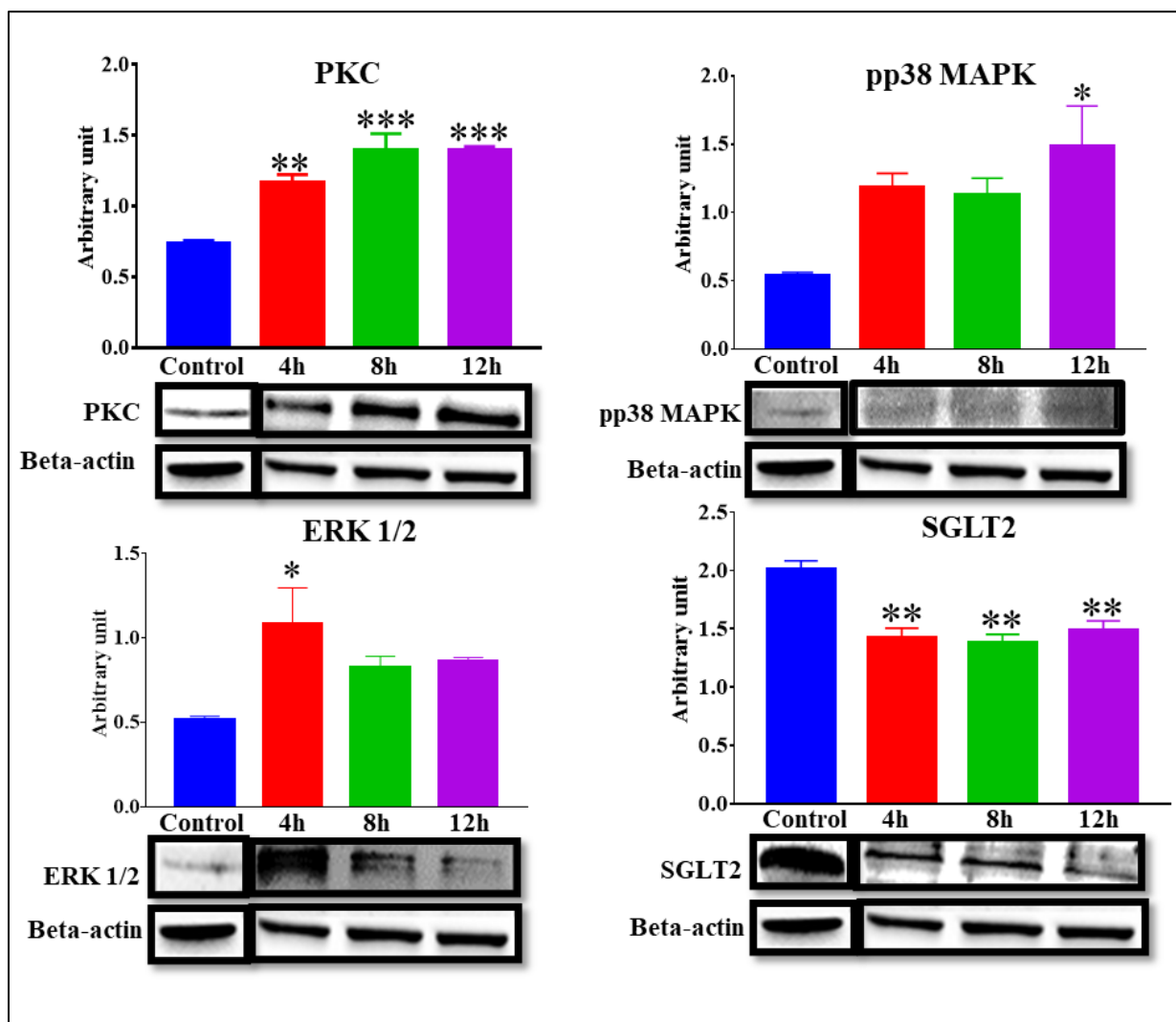


Figure 3.23 Swertisin selectively regulates SGLT2 expression. Time dependent protein expression of SGLT2 and regulating factors in the HEK293 cell line were studied. Western Blot analysis of proteins PKC, pp38 MAPK, ERK1/2, and SGLT2 along with densitometric analysis normalized to beta-actin are expressed as arbitrary unit \pm S.E.M. N=3, Significance is expressed as p-value * <0.05 , ** <0.01 , *** <0.001 control vs treatment groups

Chapter 3: Identification of molecular targets of Swertisin in glucose homeostasis, islet differentiation & functionality

3.3.3 *In vivo* molecular target identification of swertisin in glucose lowering effect

A. Swertisin improves glycaemic control in STZ induced diabetic mice: an *in vivo* study

In silico and *in vitro* results established the association of swertisin to that of SGLT2. To get a deeper understanding of SGLT2 inhibition by swertisin, we then proceeded for *in vivo* model to get insight of swertisin SGLT2 inhibitory action at a physiological level by monitoring the efficacy of swertisin in STZ induced diabetic Balb/c mice. The effect of swertisin and canagliflozin was monitored over 15 days in diabetic mice.

To check the effectiveness of STZ treatment on making *in vivo* diabetic mice model, we performed H&E staining on pancreatic section after the end of the experiment after sacrificing the mice. We observed diminished microarchitecture of islets in diabetic mice with a visibly reduced islet mass pointing towards the action of STZ on islets which acts by entering the islets by GLUT2 transporters due to structure similarity with glucose and inducing oxidative damage to the cells. Swertisin and canagliflozin treated mice exhibited normal architecture which is very similar to control mice (Fig 3.24).

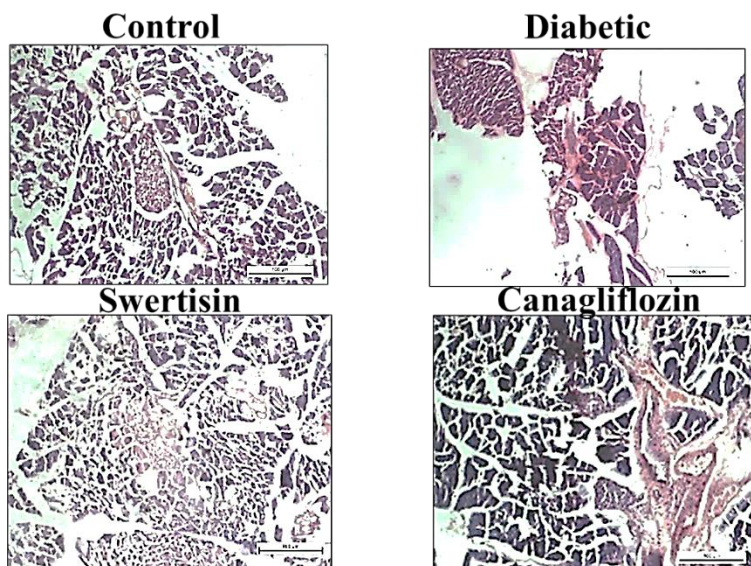


Figure 3.24 Figure showing H&E staining of pancreatic islets from control, diabetic, swertisin and canagliflozin treatment groups

Chapter 3: Identification of molecular targets of Swertisin in glucose homeostasis, islet differentiation & functionality

Swertisin dose was initiated at day 0 (326 ± 46.11 mg/dl) of treatment and reduced levels of fasting blood glucose was evident right from day 5th of treatment (253 ± 30.72 mg/dl), day 10th (230 ± 61.75 mg/dl) and persisted till day 15th (124 ± 19.08 mg/dl). Remarkably the extent of glucose lowering effect of swertisin was observed at a much lower dose (2.5mg/kg body weight) compared to positive control drug canagliflozin (10 mg/kg body weight). These results prove a higher potency of swertisin than canagliflozin for demonstrating sustainable and consistent glucose lowering effect. An oral glucose tolerance test (OGTT) was performed on Day 15th on overnight fasted mice which demonstrated controlled glycemia over the period of 2H. As predicted, OGTT results were also comparable with canagliflozin treated mice (Fig 3.25).

B. Swertisin affects physiological and metabolic parameters in STZ induced diabetic mice

In silico and *in vitro* results established the association of swertisin to that of SGLT2. We then examined several physiological parameters in all the treatment groups of mice. Inhibition of SGLT2 is expressed as changes in various metabolic parameters ultimately affecting glucose homeostasis. STZ induced weight loss in mice is commonly observed and was persistently detected in swertisin and canagliflozin treated mice. Chow intake of the Diabetic and Canagliflozin group was significantly increased compared to control mice. On the contrary, swertisin and canagliflozin groups demonstrated decreased water intake compared to the diabetic. Urine output was significantly higher in diabetic, swertisin, and canagliflozin groups with respect to control (Fig 3.26).

Chapter 3: Identification of molecular targets of Swertisin in glucose homeostasis, islet differentiation & functionality

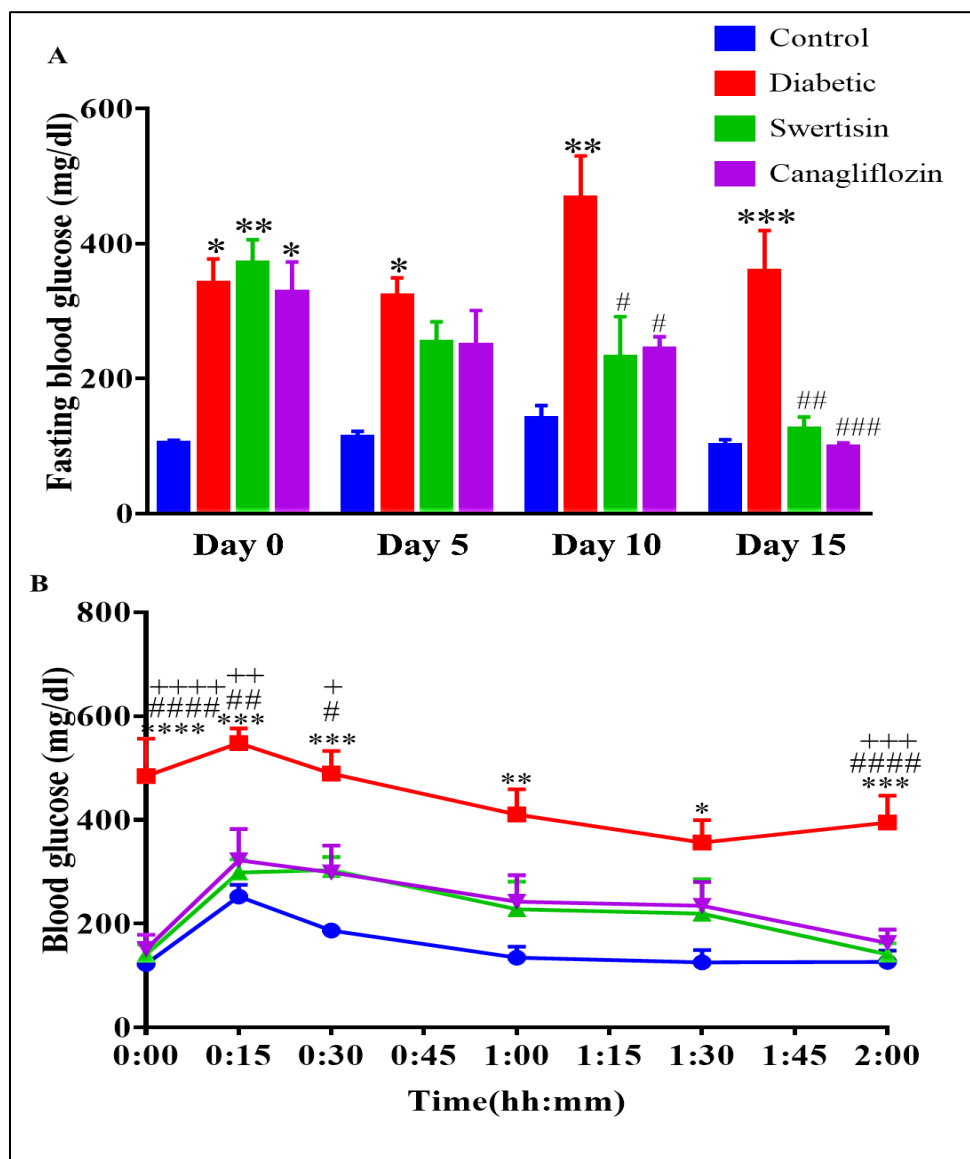


Figure 3.25 (A) Graph representing fasting blood glucose at different days of treatment for control, diabetic, swertisin and canagliflozin treated STZ diabetic BALB/c mice groups. Data are represented as mean \pm SEM. * <0.05 , ** <0.01 , *** <0.001 Control vs treatment groups # <0.05 , ## <0.01 , ### <0.01 Diabetic vs treatment groups (N=8-12). **(B)** Graph representing blood glucose levels for oral glucose tolerance test over 2H for control, diabetic, swertisin and canagliflozin treated STZ diabetic BALB/c mice. Data are represented as mean \pm SEM. * <0.05 , ** <0.01 , *** <0.001 , **** <0.0001 Diabetic vs control, # <0.05 , ## <0.01 , ##### <0.0001

Chapter 3: Identification of molecular targets of Swertisin in glucose homeostasis, islet differentiation & functionality

Diabetic vs swertisin treatment. Diabetic vs canagliflozin treatment +<0.05, ++ <0.01, +++ <0.001, ++++ <0.0001 (N=8)

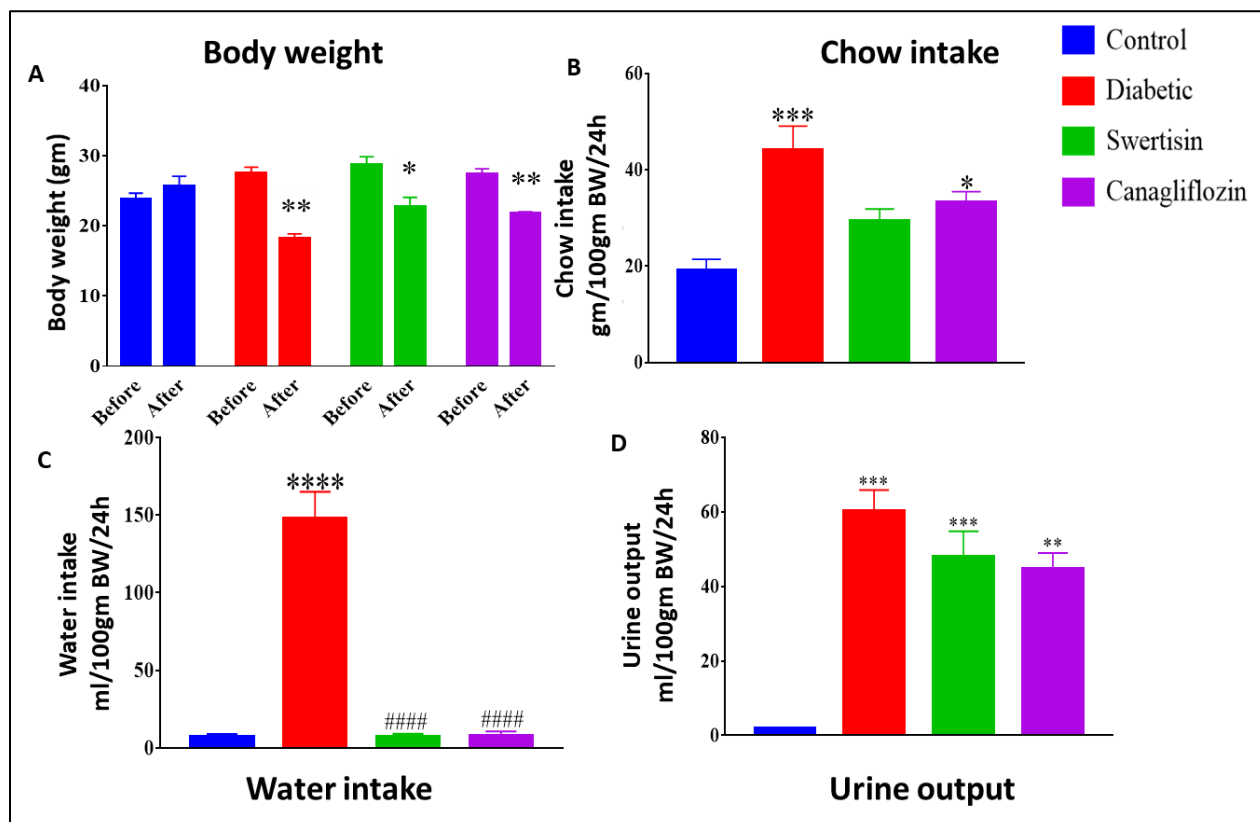


Figure 3.26 Swertisin impacts physiological and metabolic parameters in STZ induced diabetic mice Graphs representing different parameters (A) Body weight (B) Chow intake (C) water intake (D) urine output for control, diabetic control, swertisin and canagliflozin treated STZ diabetic BALB/c mice groups. Data are represented as mean± SEM. *<0.05, **<0.01, *** <0.001, **** <0.0001 Control vs treatment groups ##### <0.0001 Diabetic control vs treatment groups (N=8)

Glucosuria and proteinuria are a few of the important characteristics of diabetes (Ghezzi, Loo et al. 2018) (de Zeeuw, Remuzzi et al. 2004). Swertisin and the canagliflozin group demonstrated lesser proteinuria compared to a diabetic with the least proteinuria in the swertisin group.

Chapter 3: Identification of molecular targets of Swertisin in glucose homeostasis, islet differentiation & functionality

Glucosuria was higher in swertisin and canagliflozin groups compared to the diabetic group with the swertisin group showing the highest glucosuria (Fig 3.27).

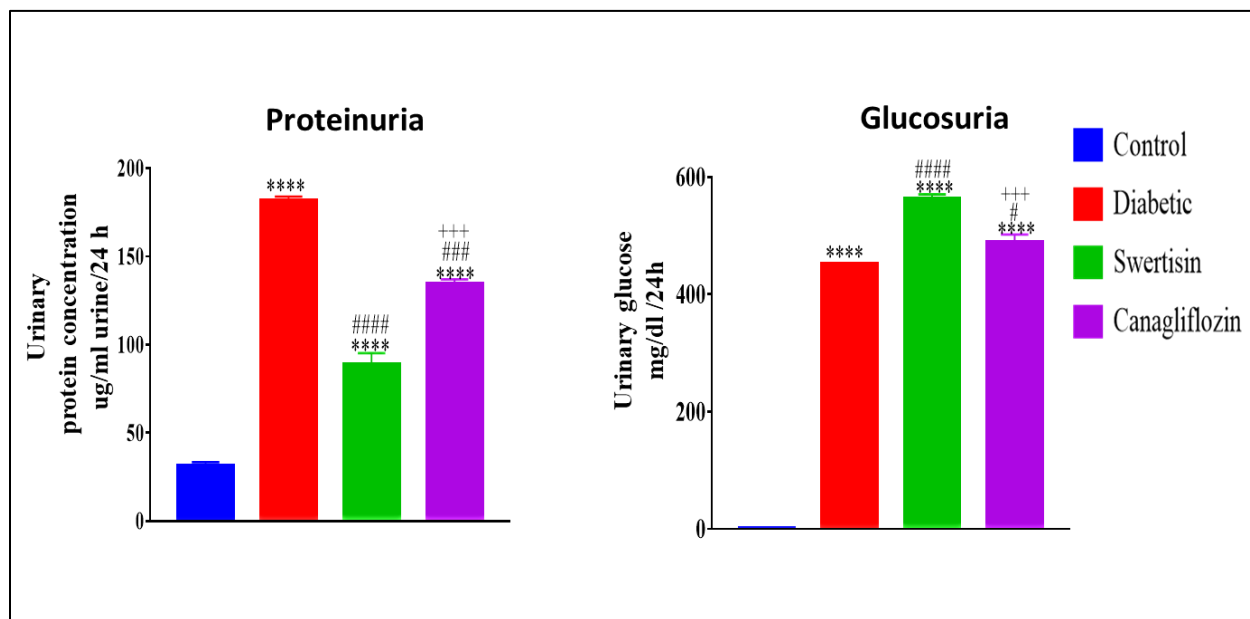


Figure 3.27 Graphs representing different parameters like proteinuria and glucosuria for control, diabetic control, swertisin and canagliflozin treated STZ diabetic BALB/c mice groups. Data are represented as mean \pm SEM. **** <0.0001 Control vs treatment groups # <0.05 , ### <0.001 , ##### <0.0001 Diabetic control vs treatment groups. Swertisin treatment vs canagliflozin treatment +++ <0.001 (N=8)

SGLT2 inhibition affects renal functions and pertains to intrarenal and extrarenal effects (Nespoux and Vallon 2018). Serum and urine creatinine levels were increased in diabetic mice compared to control mice. Creatinine clearance was higher in a diabetic with respect to control mice. Serum urea decreased in swertisin and canagliflozin treatment compared to the diabetic group (Fig 3.28). Urine urea increased in swertisin treatment compared to the diabetic group. Urea clearance increased in swertisin treatment and canagliflozin treatment concerning diabetic (Fig 3.29).

Chapter 3: Identification of molecular targets of Swertisin in glucose homeostasis, islet differentiation & functionality

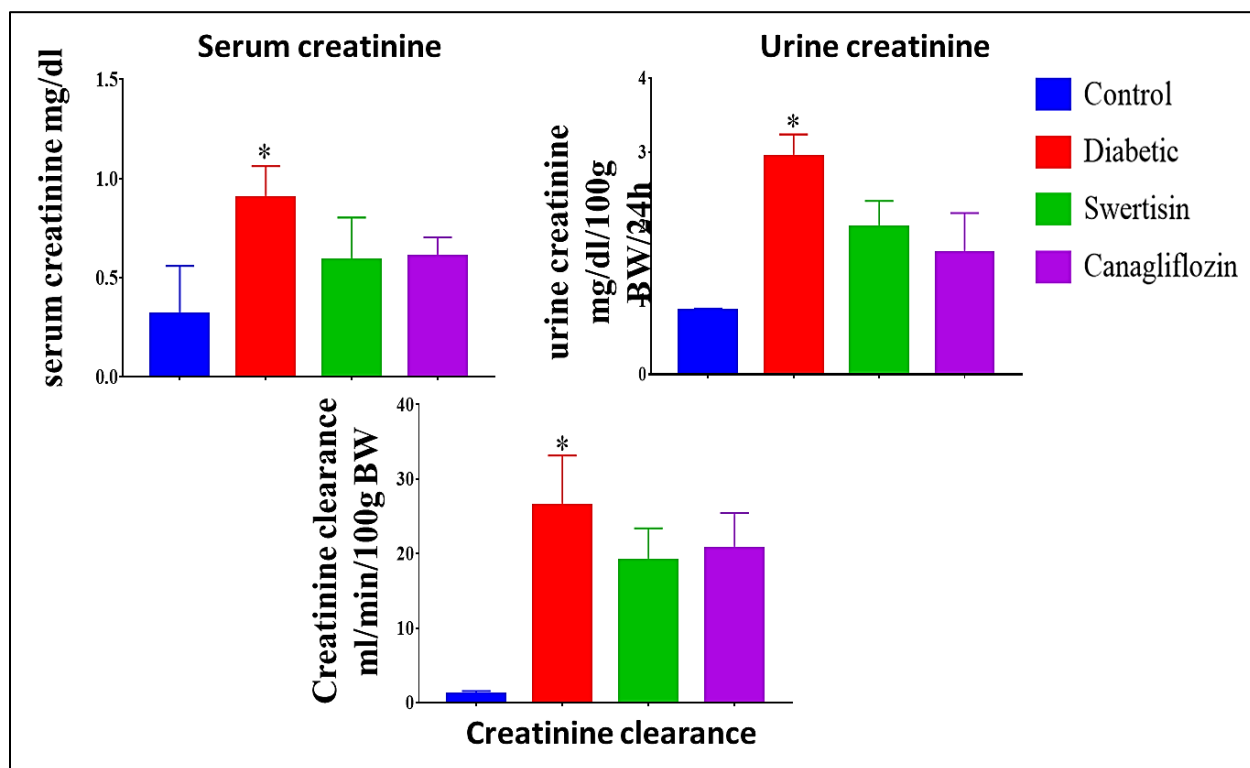


Figure 3.28 Graphs representing different parameters serum creatinine, urine creatinine and creatinine clearance for control, diabetic control, swertisin and canagliflozin treated STZ diabetic BALB/c mice groups. Data are represented as mean \pm SEM. * <0.05 (N=8)

Chapter 3: Identification of molecular targets of Swertisin in glucose homeostasis, islet differentiation & functionality

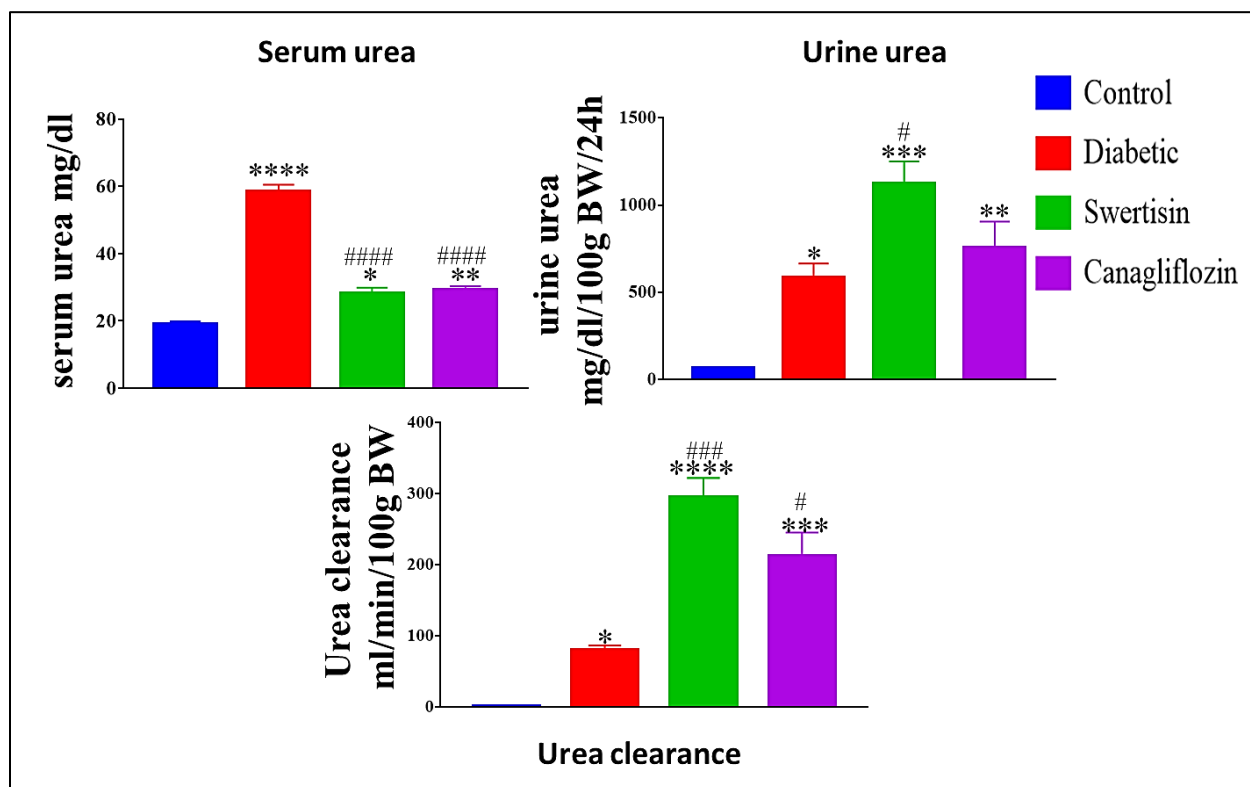


Figure 3.29 Graphs representing different parameters serum urea, urine urea, urea clearance for control, diabetic control, swertisin and canagliflozin treated STZ diabetic BALB/c mice groups. Data are represented as mean \pm SEM. * < 0.05, ** < 0.01, *** < 0.001, **** < 0.0001 Control vs treatment groups # < 0.05, ### < 0.001, #### < 0.0001 Diabetic control vs treatment groups (N=8)

C. Swertisin reduces expression of SGLT2 along with inhibition in kidney tissue of mice

Reduction in SGLT2 expression in diabetic condition has been demonstrated to improve the overall glucose homeostasis of the body by reducing the reabsorption of glucose in the blood by the kidney (Rahmoune, Thompson et al. 2005). We next addressed the question of whether swertisin affects the expression of SGLT2 in the kidney. After 15 days of treatment increased expression of SGLT2 in the diabetic and canagliflozin treated group were observed compared to control. However, the most striking result to emerge from the data is the critically reduced expression of SGLT2 which was observed in the swertisin group as compared to diabetic and

Chapter 3: Identification of molecular targets of Swertisin in glucose homeostasis, islet differentiation & functionality

canagliflozin treated mice. We also assessed PKC expression under swertisin action and favorably found that swertisin treatment not only reduced SGLT2 expression but also reduced PKC expression as well compared to diabetic. PKC was found upregulated in diabetic, swertisin, and canagliflozin groups. PKC was also found upregulated in the canagliflozin group compared to diabetic and swertisin groups (Fig 3.30). We also analysed SGLT2 expression by immunohistochemistry of kidney tissue (Fig 3.31) and found a reduced expression in the swertisin treated section as compared to diabetic and canagliflozin treatment. These results offer indisputable evidence that swertisin action involves the reduction in SGLT2 expression along with inhibition of SGLT2 action which clearly shows an advantage over canagliflozin which only inhibits the action of SGLT2 with unaltered SGLT2 expression.

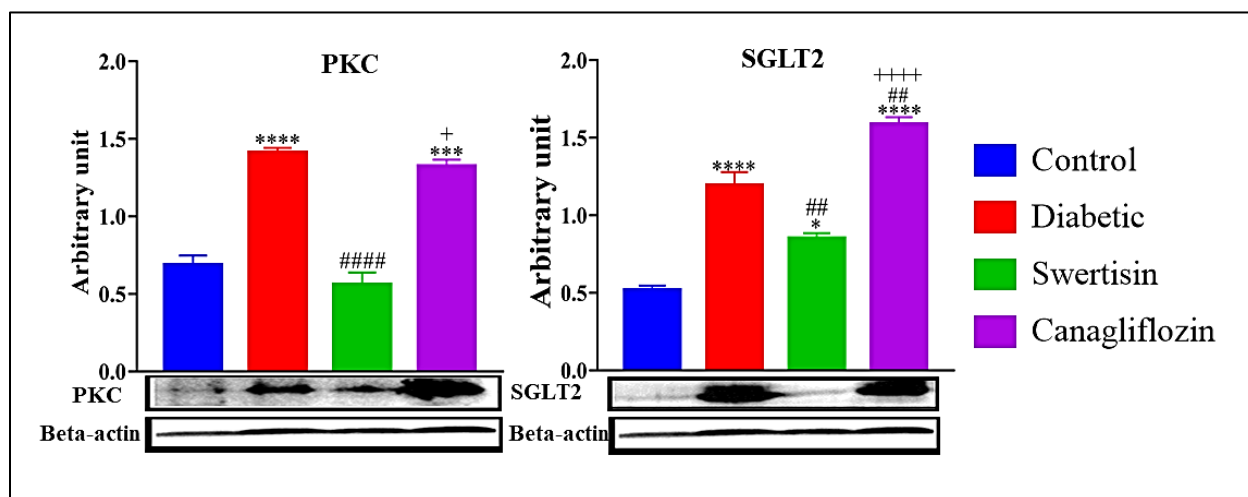


Figure 3.30 SGLT2 and PKC expression is reduced by swertisin in mice kidney. Western Blot analysis of proteins PKC and SGLT2 along with densitometric analysis normalized to respective internal control beta-actin. Data are represented as mean \pm SEM. p <0.05 , $*** <0.001$, $**** <0.0001$ Control vs treatment groups $## <0.01$, $#### <0.001$ Diabetic control vs treatment groups. Swertisin treatment vs canagliflozin treatment $+ <0.05$, $++++ <0.0001$ (N=3)

Chapter 3: Identification of molecular targets of Swertisin in glucose homeostasis, islet differentiation &
functionality

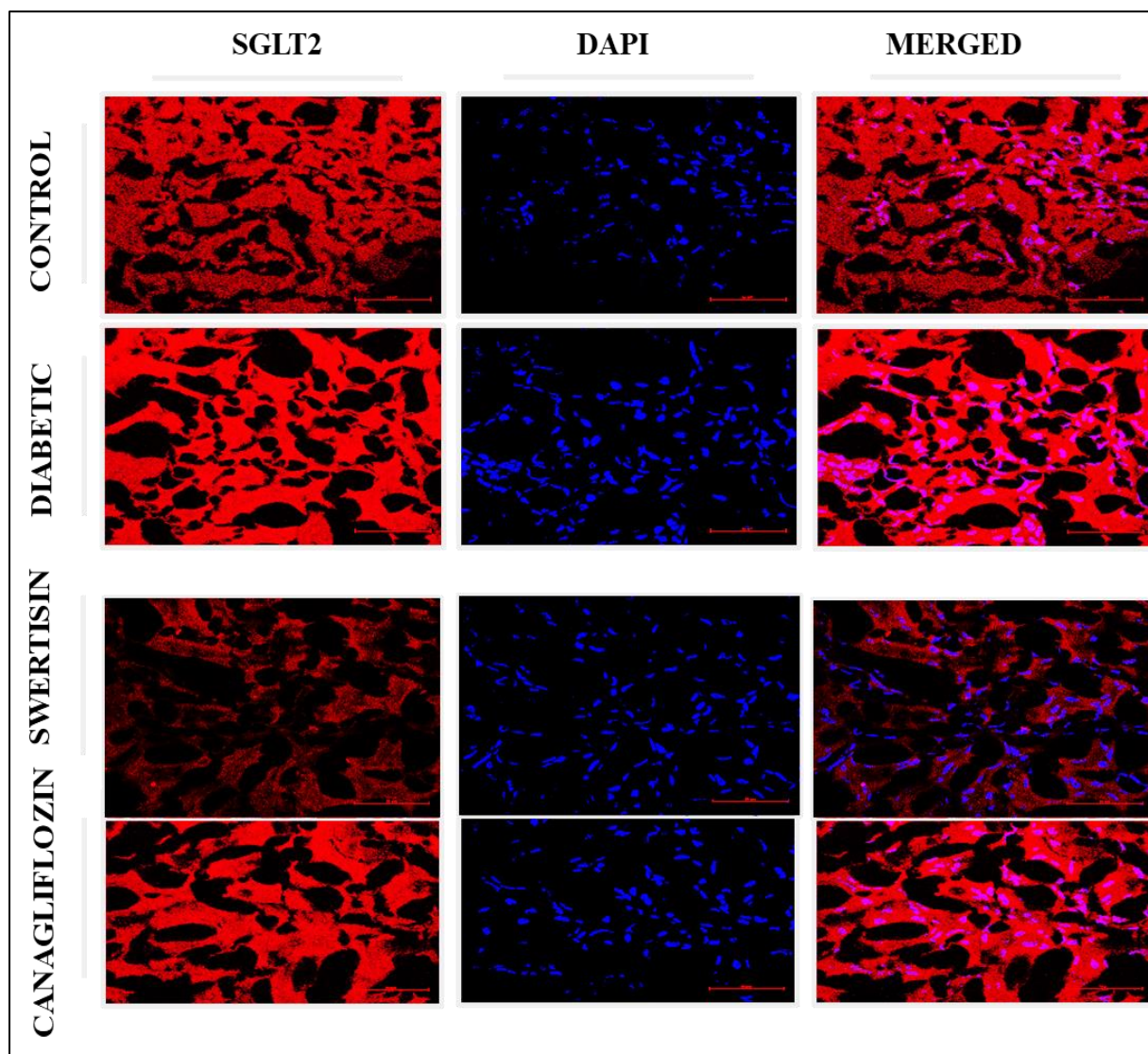


Figure 3.31 Immunohistochemistry was performed in mice kidney. Reduced SGLT2 expression was observed (N=3)

We also wanted to check any deleterious effect on kidney and intestine but found unaltered changes in the cytoarchitecture (Fig 3.32).

Chapter 3: Identification of molecular targets of Swertisin in glucose homeostasis, islet differentiation &
functionality

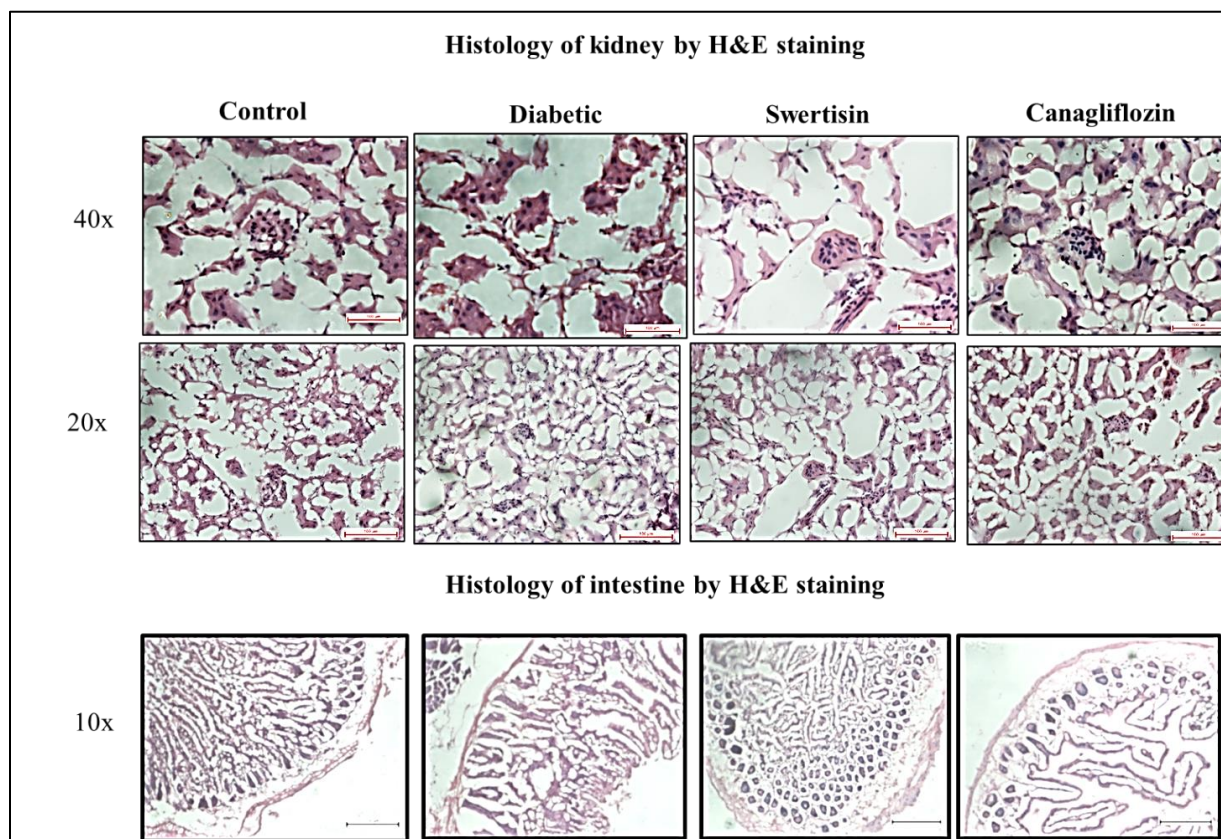


Figure 3.32 Staining of mice kidney and intestine by H&E for analysis of cytoarchitecture

Chapter 3: Identification of molecular targets of Swertisin in glucose homeostasis, islet differentiation & functionality

3.4 Discussion

The primary goal of this study was to establish the glucose lowering action of swertisin to its SGLT2 inhibition property.

Drug discovery and development are expensive and time-consuming processes. Recognition by the pharmaceutical industry that undesirable absorption, distribution, metabolism and excretion (ADME) properties of new drug candidates are the cause of many clinical phase drug development failures. To identify such problems early in the drug discovery process, *in vitro* approaches are now widely used to investigate the ADME properties of new chemical entities and, more recently, computational (*in silico*) modelling has been investigated as a tool to optimize selection of the most suitable drug candidates for development. The objectives of in-silico modeling tools for predicting these properties to serve two key aims — first, to reduce the risk of late-stage attrition at the design stage of new compounds and compound libraries; and second, to optimize the screening and testing of only the most promising compounds.

Canagliflozin is a commercially available sodium glucose cotransporter 2 inhibitor approved for the treatment for diabetes (Rosenthal, Meininger et al. 2015). The *in silico* pharmacokinetic analysis of Canagliflozin showed low absorption and high solubility. Metabolism and Elimination studies, moderate rate of metabolism and low excretion rate, which are consistent with the *in vivo* results (Devineni and Polidori 2015). Canagliflozin has dose-proportional pharmacokinetics allowing once-daily administration, and has a very limited potential to cause drug–drug interactions. Canagliflozin increases Urinary Glucose Excretion (URE) and suppresses Renal Threshold for Glucose (RTG) in a dose-dependent manner, thereby lowering PG levels and reducing HbA1c through an insulin-independent mechanism of action. Canagliflozin provides clinically meaningful reductions in HbA1c and bodyweight, and is generally well tolerated.

In silico pharmacokinetic analysis of swertisin also shows low absorption and moderate metabolism, which are consistent with the *in vivo* study where Swertisin (4.0 mg/kg body-weight) was administered intravenously in rats and the results were analysed with High-performance Liquid Chromatography-Mass Spectrometry/Mass Spectrometry (HPLC-MS/MS) method. Also, the results showed low elimination and clearance rate of Swertisin (Li, Zhao et al. 2016). Target prediction and *in silico* pharmacokinetic of swertisin shows that it is a P-glycoprotein (Pgp)

Chapter 3: Identification of molecular targets of Swertisin in glucose homeostasis, islet differentiation & functionality

inhibitor, which is coded by human MDR1 (multidrug resistance) gene. It is an energy-dependent efflux pump exporting its substrates outside of the cell. The inhibition of Pgp causes clinically significant drug retention and interactions (Tanigawara 2000). Human intestinal absorption is very poor demonstrating non-selectivity of swertisin for SGLT1 which is majorly present in intestine (Wright, Loo et al. 2011). Moreover, compared to all the other commercially available gliflozins, Swertisin shows moderate toxicity which makes it a potential candidate as a drug for treatment of diabetes.

After successful computational generation and energy minimization of human SGLT2 structure, our *in silico* data demonstrated stable molecular binding of swertisin with SGLT2 by molecular docking. Marketed SGLT2 inhibitor canagliflozin served as a comparator for our studies (Liang, Arakawa et al. 2012). Appreciably, the docking scores for Canagliflozin-hSGLT2 (-8.7 kcal/mol) and Swertisin-hSGLT2-interactions (-8.5 kcal/mol) were similar. This result strongly pointed to the likelihood of steady binding of swertisin with SGLT2.

Asp 294 of SGLT-2 is important for sugar-binding. Both luteolin and orientin, bioactive flavonoids, indicated *in silico* interaction with Asp 294 (Annapurna, Apoorva et al. 2013). Similarly, our structural docking study demonstrated that C10 atom of swertisin formed h-bond with Asp 294 which was a conserved pattern followed by canagliflozin as well.

The overall RMSD (Root Mean Square Deviation) comparison of C α backbone showed that the SGLT2-swertisin, was much more stable during the entire simulations compared to apo-protein (SGLT2) and reference inhibitor (SGLT2-canagliflozin). The radius of gyration of SGLT2, SGLT2-canagliflozin and SGLT2-swertisin shows a minor difference, which shows that the binding of ligands did not affect the compactness of the protein. Moreover, compared to SGLT2, SGLT2-canagliflozin and SGLT2-swertisin showed a lesser deviation in SGLT2. From dynamics cross-correlation matrix, it is clearly evident that residue interaction in SGLT2 was similar with that found with SGLT2-swertisin. The eigen data for SGLT2-swertisin had a steep deep indicating early stable complex formation compared to SGLT2-canagliflozin.

Bioactives aspalathin and nothofagin are the major dihydrochalcones found in rooibos (*A. linearis*). Molecular docking and MD simulations studies showed that SGLT2 inhibitors bind into

Chapter 3: Identification of molecular targets of Swertisin in glucose homeostasis, islet differentiation & functionality

the binding site of SGLT2 receptor mainly via hydrogen bonding and hydrophobic interactions. Also, both of them share similar binding energies and binding modes as dapagliflozin, a known SGLT2 inhibitor (Liu and Meng 2015).

The marked observation that emerged from our *in vitro* sodium dependent glucose uptake experiment was that the potency of SGLT2 inhibition by swertisin was significantly effective at a lower dose as against canagliflozin.

The selectivity for SGLT was confirmed by no inhibition of glucose uptake by swertisin in sodium free buffer. Inhibition of GLUT transporters leads to undesirable and adverse consequences due to the central key role of GLUT transporters in glucose homeostasis and metabolism (Jesus, Vila-Viçosa et al. 2017). Our findings confirm that swertisin does not interfere with non-sodium dependent GLUT transporters and further substantiates the selective inhibition for SGLT2 as against GLUT2 transporter.

Further, our *in vitro* experiment with HEK293 kidney cell line is in agreement with uptake results, aggregation of 2-NBDG outside the cell membrane of the kidney cell line critically confirms inhibition of SGLT2 by swertisin. This observation correlates favorably well with Ishihara et al. who reported the uptake of 3-O-methyl-D-glucose which is rapid and equilibration is 80% complete in 1 min in MIN6 cells (Ishihara, Asano et al. 1993).

Further, additional support for the selectivity of swertisin was demonstrated using the Caco2 (intestinal) cell line having SGLT1 as a major glucose transporter. SGLT1 inhibition can result in gastrointestinal side effects such as dehydration, diarrhea, and malabsorption since it is mainly expressed in the small intestine and helps in the absorption of glucose and galactose (Wright, Loo et al. 2011). As expected, we observed a non-significant change in sodium dependent glucose uptake even at higher doses of swertisin. This can be highly attributed to the C glycosylation of the swertisin structure. Compared to phlorizin and O-glucosyl analogs, C-glycosylation enables achieving higher selectivity for SGLT2 over SGLT1 and GLUT (Jesus, Vila-Viçosa et al. 2017). Panchapakesan et al. reported that SGLT1 and GLUT2 expression are unaffected by hyperglycemia and also unaffected by inhibition of SGLT2 (Panchapakesan, Pegg et al. 2013).

Chapter 3: Identification of molecular targets of Swertisin in glucose homeostasis, islet differentiation & functionality

Further we investigated regulation of SGLT2 expression under the effect of swertisin with differential expression of some protein kinases. An important observation was the reduced expression of SGLT2 protein. PKC and MAPK pathways play a major role in regulating SGLT2 under hyperglycaemic conditions (Lee, Lee et al. 2007). Upregulated PKC expression is often correlated with upregulated SGLT2 expression (Novikov and Vallon 2016). Although hyperglycemia-induced high expression of PKC was observed by swertisin treatment with downregulation of SGLT2 in *in vitro* study, it can be interpreted that swertisin does not affect PKC expression in acute treatment duration. Similarly, the expression of pp38MAPK and ERK1/2 was found to be higher. Haneda et al. lend support to high levels of ERK via hyperglycemia-induced PKC in the HEK293 cell line (Haneda, Araki et al. 1997) which summarizes the differential regulation of PKC-MAPK pathway in the kidney by swertisin.

We then moved to a pre-clinical *in vivo* animal study with some inexplicable insights. Observation of a striking reduction in fasting blood glucose of STZ treated mice by swertisin treatment substantiated our findings of improved glycaemic index. This is in good agreement with Liang et al. where canagliflozin improved glycaemic control in terms of blood glucose. Canagliflozin has also reported improved oral glucose tolerance test (Liang, Arakawa et al. 2012) which was evident for swertisin. Our finding highlights the fact that the improvement in glycaemic control by swertisin is strikingly at par with canagliflozin.

Body parameters are important for evaluating diabetogenic and metabolic parameters. Bodyweight loss in STZ induced swertisin treatment group was remarkably evident before and after treatment. Further weight loss is also aided by canagliflozin. Ji et al. further reported canagliflozin treatment increases body weight loss in diabetic mice (Ji, Zhao et al. 2017). A similar contribution of swertisin for weight management is noteworthy in our *in vivo* study.

Chow intake did not alter significantly in the swertisin group compared to the diabetic but intake was higher in the canagliflozin treated group compared to control which is also evident by Matsuba et al. who also observed that despite the increase of the calorie intake, weight loss was evident with better glycaemic control (Matsuba, Kanamori et al. 2020). Water intake was significantly lowered but an increase in urine volume in swertisin and canagliflozin groups compared to diabetic was observed as a contrast to Tanaka et al. who found that canagliflozin did not significantly inhibit

Chapter 3: Identification of molecular targets of Swertisin in glucose homeostasis, islet differentiation & functionality

water intake but also observed increase in urine volume as exhibited by diabetic patients (Tanaka, Takano et al. 2017). The most striking observation of SGLT2 inhibition is glucosuria along with proteinuria which correlates favorably well with reports (Ghezzi, Loo et al. 2018) (de Zeeuw, Remuzzi et al. 2004). Though there were differences among the control and diabetic group, the creatinine and urea levels were within normal physiological range and thus rule out the possibility of kidney dysfunction so to generate a strong possibility of effects emerging from exclusive SGLT2 inhibition which is the major focus of the study and not from kidney damage which is usually seen in chronic diabetic nephropathy models (de Zeeuw, Remuzzi et al. 2004). Thus, no nephropathic damage was observed in kidney while in H&E staining. Similar observation was made in intestine.

Renal SGLT2 expression was found upregulated in untreated diabetes in humans as well as T1DM and T2DM murine models. Higher PKC expression is found in the kidney in diabetes (Novikov and Vallon 2016). Rahmoune et al. have also observed high glucose uptake and upregulated SGLT2 expression in diabetic patients (Rahmoune, Thompson et al. 2005).

The most remarkable observation to emerge from these data was that swertisin was able to downregulate the protein expression of SGLT2 in contrast to canagliflozin. This is in good agreement with Maki et al. where they found that high glucose-induced increased expression of SGLT2 was not affected significantly by canagliflozin (Maki, Maeno et al. 2019). On the contrary, swertisin reduced SGLT2 expression which makes swertisin a better option than canagliflozin in diabetes therapeutics. Moreover, our earlier reports about potent islet neogenic property of swertisin (Gupta S, Dadheech N et al. 2010) (Dadheech, Soni et al. 2013) (Dadheech, Srivastava et al. 2015) (Srivastava, Dadheech et al. 2018) (Srivastava, Dadheech et al. 2018) (Nidheesh Dadheech Ph.D. Thesis) (Mitul Vakani Ph.D. Thesis) (Patent no. 391796 (2016) makes it even better therapeutic candidate which not only can control hyperglycemia but can also help in generating new islets, thereby combating a serious hallmark of diabetes.

Chapter 3: Identification of molecular targets of Swertisin in glucose homeostasis, islet differentiation & functionality

3.5 Summary

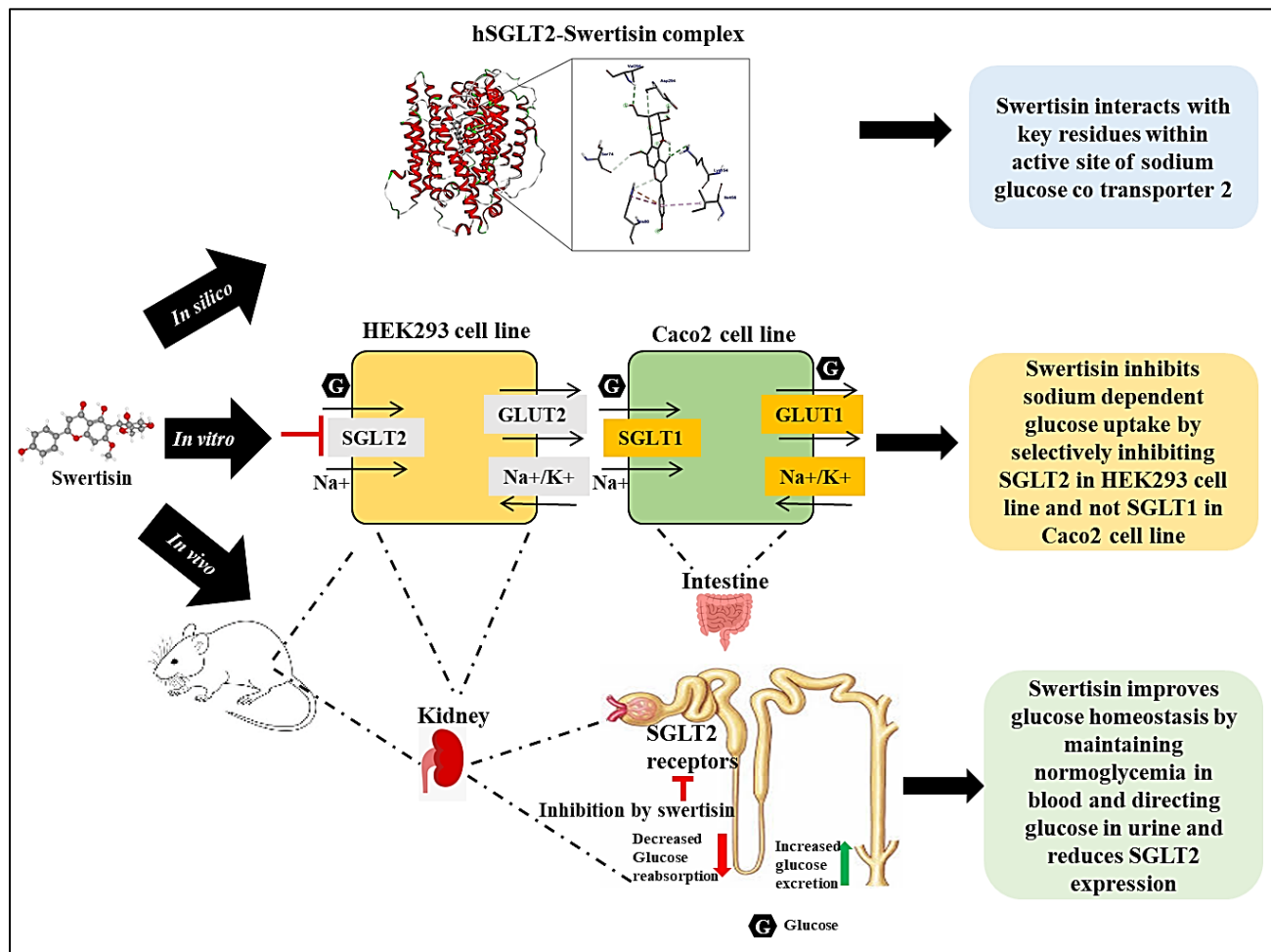


Figure 3.33 Graphical Summary of Chapter 3

Based on *in silico*, *in vitro*, and *in vivo* studies our research has highlighted the importance of SGLT2 inhibition and its reduced expression by swertisin. The direct role of swertisin in controlling hyperglycemia makes it an excellent pharmacophore agent that can ease the burden of diabetes healthcare management by providing holistic treatment and a foremost candidate for SGLT2 inhibitors (Fig 3.33).

Chapter 3 is published in ‘Archives of Biochemistry and Biophysics’ Journal.
(Full length paper can be found in the ‘Publications’ section of the Thesis)

